Open File Report OF98-3

Enzyme Leach and Mobile Metal Ion B-Horizon Soil Geochemical Signatures of Buried Geophysical Conductors, Assean Lake Area, Northeast Manitoba

Manitoba
Energy and Mines

David Newman
Minister

Manitoba
Energy and Mines
Geological Services

Open File Report OF98-3

Enzyme Leach and Mobile Metal Ion B-Horizon Soil Geochemical Signatures of Buried Geophysical Conductors, Assean Lake Area, Northeast Manitoba

by M.A.F. Fedikow and D.V. Ziehlke*
Winnipeg, 1998

* Strider Resources Ltd., Snow Lake

GEOREF

NTS AREA: 64A/1NW

Keywords: enzyme leach
mobile metal ion process
Hunt claims
base metal
precious metal
Assean Lake, Manitoba

TABLE OF CONTENTS

FIGURES

TABLES

SUMMARY

Twenty-two B-horizon soil samples were collected at 50 m stations along one transect oriented perpendicular to the interpreted bedrock axis of a long strike length ground electromagnetic (EM) conductor in the Assean Lake area (Fig.1). The conductor is flanked to the north and south by shorter EM conductors. B-horizon soil samples were analyzed by inductively coupled plasma-mass spectrometry (ICP-MS) subsequent to dissolution using the enzyme leach and mobile metal ion (MMI) processes. High contrast multielement multi-sample geochemical anomalies were identified over the long strike length ground EM conductor that is topped by 11 m of wet peat and lacustrine clay and 25 m of non-mineralized bedrock. Lesser responses were obtained from the adjacent or flanking conductors. Enzyme leach elements Cu, Pb, Zn, Ni, Co, As, rare earth elements (REE), Zr, Y, Nb, Ba, Rb, Sr, U, Th, Se, Li, Sc, V and Mn delineated the main conductor as did non-transformed data and calculated response ratios for mobile metal ion elements Co, Cu, Ni, Pd, Zn, Ag, Au and Cd. Diamond drill core logs and assay information indicate the main conductor is characterized by a 12 m thick mineralized zone with higher grade intersections of up to 7.1% Zn, 2.2% Pb and 715.4 grams per tonne Ag over 0.2-0.8 m. The deposit is interpreted to be of the sediment-hosted massive sulphide type. Exploration on the property undertaken subsequent to mobile metal ion surveys resulted in the intersection of up to 5.1% Zn, 1.6% Pb, 0.4% Cd and 28.8 g/t Ag in a base metal massive sulphide type depositional environment. Additionally, a chert or ultramylonite-hosted zone of 22.2 g/t Au and 190 g/t Ag was also discovered. Both of these types of deposits had been indicated by the original Hunt transect enzyme leach and mobile metal ion surveys. The success of both analytical approaches in identifying and differentiating the main conductor from other conductors in the area indicates the potential for application to mineral exploration in the Assean Lake area where bedrock is concealed by thick and compositionally variable surficial deposits. Follow-up mobile metal ion surveys have substantiated the results from the orientation program.

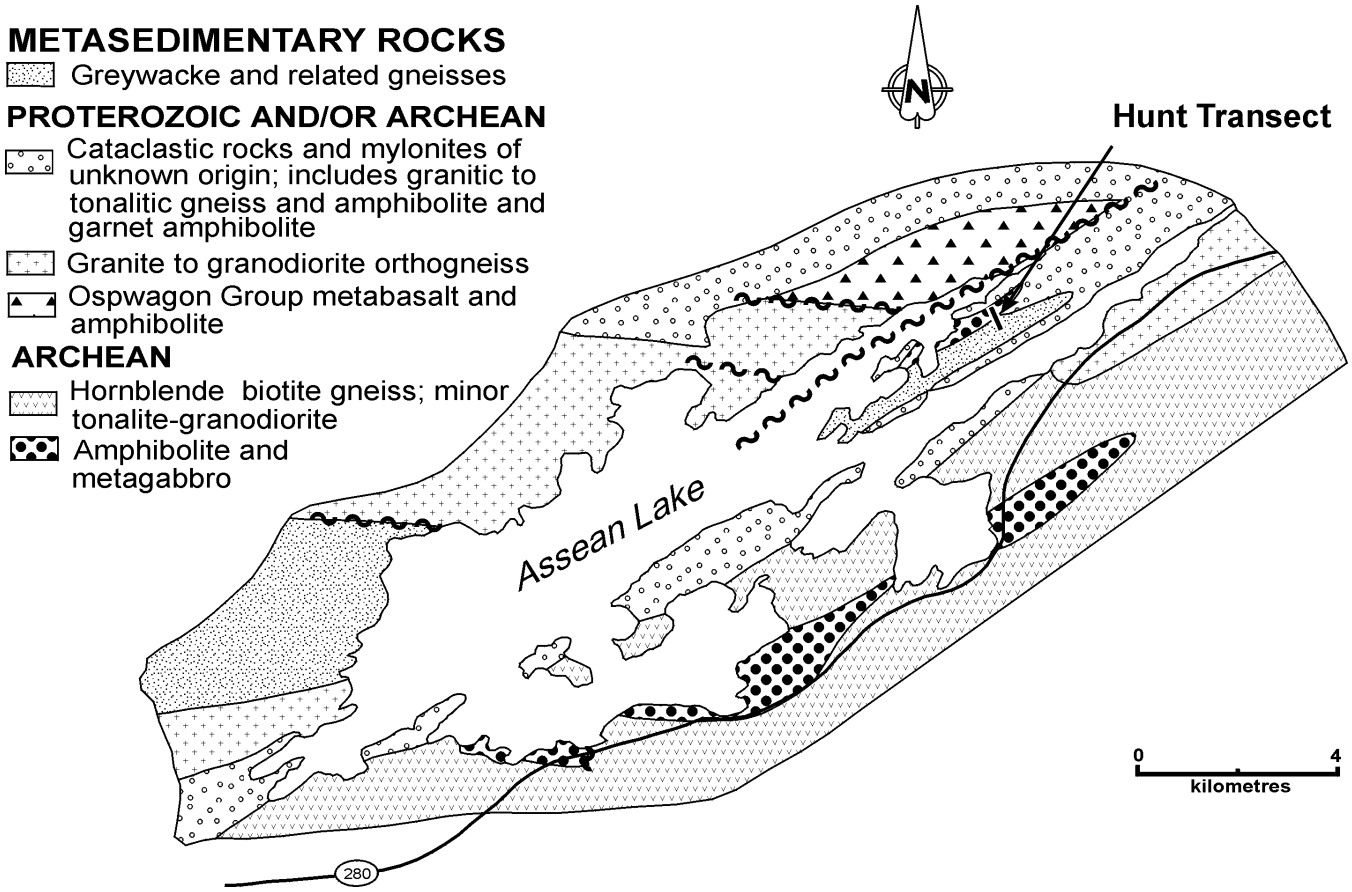

Figure 1: Geological setting of the Assean Lake area (modified after Haugh, 1969).

INTRODUCTION

Surficial deposits, such as till, lacustrine sand, silt, clay and peat represent serious impediments to mineral exploration. Although the analysis of various size fractions of glacial till and to some degree boulder tracing, has been successful in delineating gold- and base metal-enriched heavy metal dispersion fans, the explorationist is still required to search "up-ice" or within the areal influence of these dispersion trains for the source of the anomalies. In some instances, the till dispersion fans can attain considerable areal dimensions (cf. Kaszycki, 1989). The recent development of geochemical techniques based on sequential, phase specific and partial digestions coupled with analytical technological advances that permit routine parts per billion analysis has provided an opportunity to "see through" transported and other types of overburden. Anomalies defined in this manner generally occur directly over, or in the immediate vicinity of the mineralized source. The enzyme leach and mobile metal ion (MMI) approaches to geochemical prospecting represent two commercially available techniques that have application to blind and/or buried mineralization. Researchers responsible for the development of the MMI approach indicate that a geochemically anomalous response is only obtained over a mineralized zone where "significant" amounts of metals are present. Accordingly, this may permit ranking or prioritization of airborne or ground geophysical conductors for follow-up drill testing, thereby avoiding expensive assessment of "barren" sulphide facies iron formation. These two analytical techniques formed the basis for the orientation survey conducted over the Assean Lake conductive zones.

GEOLOGICAL SETTING OF THE GEOPHYSICAL CONDUCTORS

The Assean Lake area straddles the boundary zone between the Superior and Churchill geologic provinces (Fig.1). This structure has been termed the Superior Boundary Zone (SBZ). Geology is characterized by a major zone of cataclasis developed within a compositionally and texturally diverse suite of gneisses intruded by felsic to mafic intrusions. Metallogenetically, the SBZ is host to the important Ni-Cu deposits of the Thompson nickel belt (TNB). Additional information on the geology, geochemistry, geophysics and exploration potential of the TNB is available in McRitchie (1995).

The EM conductors that represent the targets for this survey occur within a unit of hornblende amphibolite and chert interlayered with greywacke (Fig. 2). More detailed geology in the area is inferred from exploration oriented geophysical surveys (Homestake Mineral Development Company, 1985) and extrapolation of geology from lakeshore exposures and limited diamond drilling by Hudson Bay Mining and Smelting Co., Limited.

Subsequent to the initial interpretation of the enzyme leach and mobile metal ion surveys, diamond drill information from exploration of the EM conductors by Hudson Bay Mining and Smelting Co., Limited in 1965 was obtained. Diamond drill hole Tex 17 intersected a 14.2 m (46.2') mineralized interval of up to 15% sulphide mineralization characterized by disseminated pyrite, pyrrhotite, sphalerite and galena. Within this mineralized zone higher grade intersections of up to 7.1% Zn, 2.2% Pb and 715.2 grams per tonne Ag over maximum core widths of 0.2-0.8 m were identified. Host rocks to the mineralization are biotite schists and quartz-biotite-plagioclase gneiss. Both lithologies contain narrow bands of chlorite schist. This mineralized zone is represented by the long strike length ground EM conductor tested with the enzyme leach and mobile metal ion methods.

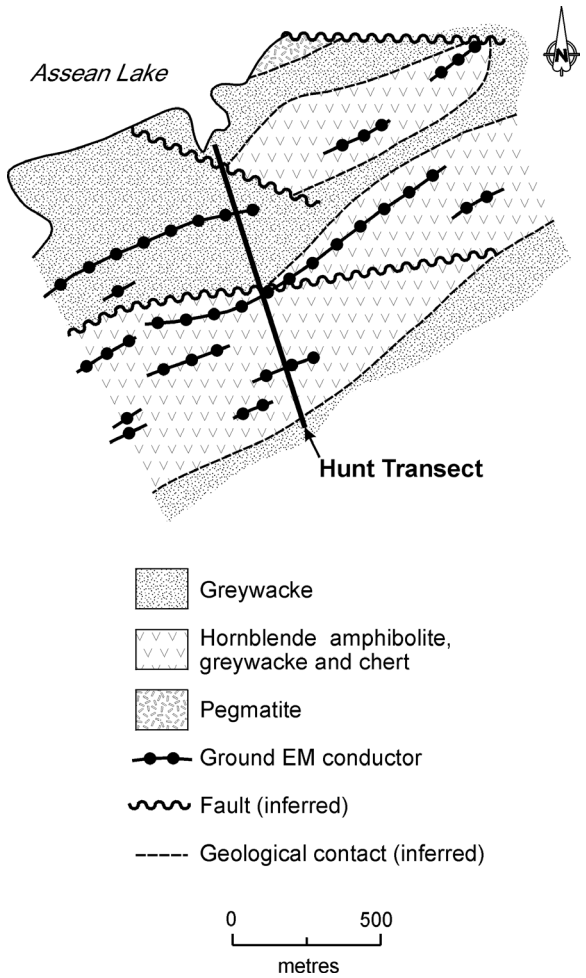

Figure 2: Local geology of the survey area (modified from assessment file 93431).

QUATERNARY GEOLOGY

Outcrop in the immediate area of the conductors is scarce owing to a cover of massive and varved clay, sand and silt locally topped by wet peat. The inorganic sediments are glaciolacustrine deep basin deposits that form extensive plains and discontinuous veneers in the Assean Lake area. Surficial deposits along the soil sampling transect consist of a variably coloured silty clay, representing the B-horizon, topped by black to brown, poorly to moderately decomposed humus with root mat. The B-horizon generally occurs at depths of less than 0.4 m. Depth to bedrock is unknown but was initially estimated from shoreline exposures to be 10-15 m. Overburden descriptions and depth to bedrock obtained from old diamond drill core logs indicate a thick lacustrine and glaciolacustrine cover. Descriptions from the drill holes that penetrated the mineralized ground EM conductor and/or were abandoned in the immediate area of the conductor are as follows:

DDH 17:0-2' muskeg; 2'-38' (11 m) lacustrine clay resting on bedrock
DDH 26 (abandoned):0-30' (9 m) lacustrine clay; 30'-98' (21 m) sand, gravel and boulders
DDH 28 (abandoned):0'-34' (10 m) lacustrine clay; 34'-88' (17 m) sand, gravel and boulders
DDH 31:0-48' (15 m) lacustrine clay resting on bedrock
DDH 34:0-34' (10 m) lacustrine clay resting on bedrock

The upper or active layer is characterized by lichen, an assortment of grasses (*Salix sp*.), and blueberry (*Vaccinium augustifolium*) and labrador tea (*Ledum groenlandicum*). In areas of ponded water the active layer was characterized by 0.25 m of sphagnum and variably humified blonde to dark brown peat. Permafrost was locally encountered at about 0.5 m. Groundwater characteristics in the study area are unknown.

SAMPLE COLLECTION AND PREPARATION

A total of 22 B-horizon soil samples were collected from hand-dug pits on the sampling transect. Samples were collected from stations 50 m apart and consisted of approximately 2 kg of inorganic silty clay B-horizon material and stored in medium sized ZIPLOC freezer bags. B-horizon was encountered at an average depth of about 40 cm. Care was taken to exclude all organic material from the sample. Since sampling was undertaken in late September ambient air temperature was constant at approximately 15° C. Possible volatilization of metal-bearing compounds from the H_2O-rich amorphous manganese oxide coatings was thereby avoided. Sample preparation was undertaken in the laboratories of the Geological Services Branch. Samples were air dried on plastic, disposable plates, split into two equal portions with one portion sieved to obtain the -60 mesh size fraction. The -60 mesh fraction was forwarded to Activation Laboratories Ltd. (Ancaster, Ontario) for multi-element ICP-MS analysis subsequent to enzyme leach extraction. The second sample split was sieved to obtain the -80 mesh size fraction and forwarded to XRAL Laboratories (Toronto, Ontario) for analysis using the MMI process.

SAMPLE ANALYSIS

I. Enzyme Leach

This process is a phase-specific leach that preferentially attacks amorphous manganese oxide coatings on mineral grains thereby liberating trace metals that are trapped in this material. Amorphous manganese oxide represents an efficient chemical sieve or trap for cations, anions and polar molecules because of its large surface area and the random distribution of charges on its surface. The trace elements that are trapped or complexed on the amorphous manganese oxides are interpreted to represent the chemical signatures of buried, oxidizing mineralization at depth, rather than signatures originating from a transported overburden source, such as till.

It should be noted, however, that where B-horizon development takes place in till the geochemical signature within the B-horizon may be strongly affected by the weathering of till and the subsequent downward movement of metals as a result. This could produce a "transported" till geochemical signature in combination with site specific mineralization-related geochemical signatures and a composite signature overall. The possible contribution of parent sediment composition to the overall enzyme leach signature is not well understood.

Most of the amorphous manganese oxide is developed in the B-horizon, where studies in both arid and humid geological and climatic environments have established that mineral particles within this soil horizon are coated with this authigenic material. The A-soil horizon may not reflect geochemical anomalies identified in the B-horizon since A-horizon may be fairly rapidly leached of its metallic components which are carried downwards, perhaps as humic- or fulvic-acid compounds (humates/fulvates?), and trapped or sieved as they encounter the amorphous Mn-oxide coatings on mineral grains in the B-horizon. The chemical composition of the A-horizon can be significantly impacted by the metal contents of vegetation contributing litter to the forest floor. This litter will reflect metals obtained by vegetation during nutrient

acquisition from soil horizons tapped by root systems. Accordingly, the A-horizon geochemical signature can reflect the ability of various species to acquire and store metals until such time as they are dropped to the forest floor, decompose and move downward in the soil profile. This source of metal may therefore reflect a transported metal signature representing a clastic component within an exotic till at depth rather than a buried mineralization signature.

The diffusion of relatively volatile metal phases or metal transport by gases consisting of Hg-vapour, CO_2, Rn, He, N, O_2, CO_4 , Ar and S-compounds, away from an oxidizing zone of mineralization, undoubtedly proceeds as a result of a number of processes. Metal transport may be effected by the influence of an electrochemical or self-potential cell, or possibly as components in soil gases derived from mantle de-gassing (cf. Gold and Soter, 1980; "geogas", Malmqvist and Kristiansson, 1984; "earth-gas", Wang et al., 1997). The role of shallow groundwater as the transport medium for metals from source to surface is also being investigated (Stewart Hamilton, pers. comm., 1998). Metals carried by one or more of these mechanisms will enrich the amorphous Mn-oxide in the B-horizon in metals. Native gold and mercury in the soil profile will not be digested using the enzyme leach.

The leachate from the B-horizon soil is analyzed by ICP-MS for 59 elements at detection limits in the parts per billion range. Clark (1992, 1993) provides theory and application of the enzyme leach method.

II. Mobile Metal Ion Process

This process was developed in Western Australia by a consortium of exploration companies seeking tools to geochemically "see" through residual overburden. A weak partial extraction scheme is used on a 100 g sample of soil to liberate ions which have been mobilized to the surface from buried or blind mineralization where they become loosely bound to soil particles. For the purposes of the Assean Lake survey the target soil sample was collected from the B-horizon so that a comparison to the enzyme leach results could be made. Separate dissolutions or extractants are used and provide a leachate for a base metals package (Digest A for Cu, Pb, Zn and Cd) and a precious metals package (Digest B for Au, Ag, Ni, Pd and Co). This leachate is then analyzed by ICP-MS for a multielement suite in the parts per billion concentration range.

The exact chemistry of the multi-component dissolutions is unknown owing to proprietary considerations. Available literature citations indicate MMI anomalies are well defined and usually overlie the mineralized zone, thereby defining the vertical surface projection of the mineralization. Numerous case histories have been undertaken in a variety of geological environments and document the effectiveness of this technique. A general description of the method is provided by Birrell (1996).

RESULTS

Enzyme leach and MMI data from the Hunt B-horizon sampling transect are displayed as profiles and as response ratios for the MMI data. The locations of the main and lesser EM conductors, and an inferred fault are plotted on the profiles. The enzyme leach elements Be, Ru, Rh, Ag, In, Sn, Te, Re, Os, Ir, Pt, Au, Hg, Tl, and Bi are below the lower limits of detection (LLD) and are not discussed further. Some elements are primarily at or only slightly above the LLD, however, the few analyses for these elements that are above the LLD are invariably sited over the ground EM conductor or the associated fault. These elements include Ti, Ga, Ge, Se, Pd, Cd, Sb, Cs, Eu, Tb, Ho, Er, Tm, Lu, Hf, Ta and W. A selection of the profiles derived from some of these elements (Se, Pd, Cs, Lu, Ta and W) are presented in the following discussion.

Analytical data for enzyme leach field duplicates and transect samples are presented in Appendix 1. Enzyme leach profiles are reproduced in Appendix 2.

Enzyme Leach

Analytical Reproducibility

A rigorous assessment of enzyme leach field duplicate reproducibility is not possible since only two duplicate pairs were collected along the 22 sample transect. Generally, most elements above 10 ppb vary within ±25%. Chlorine appears to be the least reproducible of the elements greater than the lower limit of detection (LLD). Analyses at sub-20 ppb concentrations are less reproducible since slight sample inhomogeneities, fluctuations in instrument stability or digestion procedure can impart significant variance to the data.

Geochemical Signatures

Main Conductor

The major, long strike length ground EM conductor is characterized by readily identifiable, high contrast responses for Cu (>200 ppb), Pb (>20 ppb), Ni (200 ppb), a consistent REE (La, Ce, Pr, Gd, Tb, Dy, Nd, Sm, Yb) signature often in the hundreds of ppb, Zr (>450 ppb), Y (>160 ppb), Nb (8 ppb), Ba (>1500 ppb), Rb (>65 ppb), Sr (>850 ppb), Th (120 ppb), Li (>150 ppb), Sc (>100 ppb), Ta (2 ppb), Mn (1800 ppb), and Cs (2 ppb).

Arsenic has a non-definitive sawtooth pattern and Co is marked by a number of "spikes" varying in concentration between 30-44 ppb over a 200 m portion of the sampling transect which includes both the main conductor and the inferred fault that occurs 100 m to the south. The geochemical coherence of the REE is reflected by the similarities in their responses.

Inferred Fault

The inferred fault that is transected 100 m south of the main conductor at Point B is without a ground EM signature but nevertheless has a distinctive multielement geochemical signature. Zn (>60 ppb), Pb (>15 ppb), Co (44 ppb), Zr (>500 ppb), Nb (7 ppb), Rb (>80 ppb), Sr (>700 ppb), U (>25 ppb), Th (>80 ppb), Li (>140 ppb), Sc (>70 ppb), V (>500 ppb), Cs (2 ppb), and Mn (>1100 ppb) all form peaks on this structure. Generally, the base metal response is lower over the fault than over the main conductor at Point B.

Mo-Se-Te Response (Gold-Bearing Dunbrack Structure?)

The geochemical response of these three elements may be significant in that they delineate a Mo-Se-enriched (and perhaps Te-enriched albeit at lower concentration levels) zone between 0 and 200 m on the sampling transect. Selenium (69 ppb) and Te (1 ppb) form peaks over the main conductor. A single sample Se response (85 ppb) and the 5 sample Mo signature (10-16 ppb) are situated close to the lakeshore of Assean Lake and approximately along strike from the shear-hosted Dunbrack and Lindal Au occurrences (Fedikow and Ziehlke, 1996). Alternatively, the responses are attributed to a lesser ground EM conductor at 200 m.

Subsidiary Conductors

High contrast V and Mn responses were obtained over each of the three conductive zones, including the main and the subsidiary conductors, as well as the inferred fault 100 m south of the main conductor. These peaks clearly identify each of the targets; the geochemical signals from the flanking conductors are somewhat lower. Other responses include low Cs (1 ppb), W (2 ppb), U (5 ppb) and Zn (>40 ppb) and significant anomalies for Se, Mo and possibly Te associated with the ground EM conductor (and/or the associated fault) at 200 m on the transect.

Morphology of the Enzyme Leach Geochemical Responses

The shape or morphology of the enzyme leach-based geochemical signatures are apical although a rabbit-ear or doubly-peaked response is apparent if the signatures of the main conductor and the inferred fault are combined. The apical responses are primarily single-peaked, high contrast responses developed directly over the EM conductors and the adjacent inferred fault. Some shift in anomaly location in relation to the conductors and the fault is noted but this may be related to a small error in the plotting of the surface projection of the EM conductor or of sample sites along the transect rather than a fundamental cause and effect relationship. It should be remembered that good control of the geology of the area is lacking due to the surficial cover.

Mobile Metal Ion

Interpretation of the MMI data is based upon the examination of non-transformed MMI analyses and calculated MMI response ratios. Response ratios are derived as per the recommendations of the developers of the MMI process. For each element of interest a background is calculated by determining the 25th percentile or the lowest quartile. A peak to background ratio or response ratio is then determined by dividing all analyses by the average of individual values, considered to represent the background, within this quartile. Benefits from this normalization include: (1) a reduction in the effects of dissolution variables such as time and temperature during extraction; (2) a reduction in the effects of sample error in different regolith environments; (3) facilitate data integration from samples collected in different regolith environments; and (4) facilitate multielement data presentation for the purpose of interpretation. Response ratios are then plotted as individual or stacked bar charts. Individual element bar charts are used for interpretation in this survey. For purposes of background calculation all values less than the lower limit of detection were replaced with a value one half of the detection limit.

Appendix 3 contains analytical data for the mobile metal ion process including field and analytical duplicates. MMI profiles and response ratio plots are presented in Appendix 4.

Duplicate Sample Analyses

Field duplicate pair reproducibility for Cu and Zn from the 450 m sample station on the transect are suspect. Pb, Zn and Cd are also poorly reproduced from the 900 m site. Nickel, Co and Ag appear to be reproducible at their observed concentration levels. Analytical duplicate pairs show excellent reproducibility with the exception of Pb which was the only MMI element that did not identify the conductive and/or the structural zones.

Interpretation of Non-transformed Data

The area between 500 and 650 metres on the sampling transect is highlighted by multiple base and precious metal responses. In the area of the surface projection of the main EM conductor and the inferred fault Au (37 ppb), Ag (20-74 ppb), Pd (53 ppb) and Co (45-129 ppb) produce high contrast responses. Cu (22-1240 ppb), Zn (64-236 ppb) and Cd (25-30 ppb) peaks are also noted over this portion of the transect. The Ni response forms a multiple sample (n=5) rabbit-ear anomaly varying from 416-1300 ppb between 500-550 m to 5 ppb at 600 m to 622-1910 ppb between 650-700 m. The "sawtooth" Pb response is considered to be non-definitive. The Pd, Zn, Au peaks, and to a lesser extent the Co and Cd peaks appear to be centered over the inferred fault and may be related to mobilization of metals into post-depositional structures. The form of the Co, Ag and Ni responses approximates a "rabbit-ear" signal while all other elements form apical or single peak responses. Lesser responses for Co, Ag and Ni are observed over the weak or flanking ground EM conductors on the profile at 200 and 950 m. A moderately high Cd response (22 ppb) is obtained between 0 and 100 m. Cu, Pb and Ag peaks are developed 50 m north of the Zn, Cd, Au and Co peaks and as such are suggestive of metal zonation at source.

Interpretation of MMI Response Ratios

Individual plots of MMI response ratios basically provide the same information as non-transformed MMI analytical data. The long strike length ground EM conductor and the inferred fault, as well as the portion of the transect between these two features, are identified as multielement geochemically anomalous sites. Response ratios for Au (as well as Au in non-transformed MMI data) identify an anomalous response over an inferred fault at 600 m on the transect.

Follow-Up Surveys and Exploration Results

Subsequent to interpretation of the enzyme leach and MMI responses obtained from the Hunt transect, B-horizon soil samples were collected from additional lines on the Hunt property (Fig. 3 in pocket) to assess ground EM responses and magnetic anomalies. Analytical data are presented in Appendix 5 and results for field and analytical duplicates in Appendix 6. Response ratios were calculated for these data and presented in Appendix 7.

Results

Analytical duplicates for MMI elements (Appendix 6) in the follow-up survey are excellent. Field duplicates from sites 51 and 52 exhibit significant variance. Despite being collected less than 10 m apart these two samples have vastly different colour and textural characteristics. Sample 51 was an oxidized, reddish brown pebbly clay whereas sample 52 was a light beige "sticky" clay collected directly from the top of a subcrop of unknown composition. These differences may account for the significant differences for Cu (441 vs. 171 ppb), Zn (91 vs. 10 ppb), Pb (68 vs. <20 ppb) and Ni (129 vs. 39 ppb). Silver appears unaffected by this compositional difference with duplicate pair results of 19.8 and 15.3 ppb.

Elevated mobile metal ion responses are documented in proximity to ground EM conductors on each of the four lines sampled during the follow-up survey. Copper, Pb, Co and Ni apical responses occur at approximately 300 m on line 14E and correspond to a ground EM conductor. The Zn response ratio at this location is a doubly peaked anomaly with a trough of low response ratios over the conductor. Complex, repetitive folding documented from exploration on the property may explain the "rabbit-ear" anomaly rather than an electrochemical mechanism of dispersion. The EM conductors at approximately 540 m and 630 m could not be assessed due to the lack of inorganic B-horizon soil samples. The conductors occur in swamp. Generally low Au response ratios (3) were observed on this transect. A high Ni response occurs near the 800 m portion of the transect.

A Cu-Zn-Pb-Co response was observed at 330 m on line 19E, however, there were no elevated responses directly over the ground EM conductor on this line. The ground EM conductor on line 23E is marked by a Zn-Cu-Pb-Ni response with an associated, albeit low, Au response ratio of 3. A moderate Co signature (response ratio=10) is documented from the 300 m section of the transect. A strong Cu response and an associated lesser Pb response occurs at 200 m on line 29E and corresponds to the location of the EM conductor on this line.

Comparison of Elevated Response Ratios and Diamond Drill Results

Table 1 summarizes significant response ratios from each of the four lines that were sampled and Table 2 reproduces significant assay intervals from follow-up diamond drilling of coincident airborne magnetic and ground EM anomalies as well as mobile metal ion responses. The most significant MMI results are those from line 14E where a strong base metal signature was isolated. This response was one of two MMI anomalies tested by diamond drilling during this exploration phase.

The apical Cu-Pb-Co responses and the multiple peaked responses for Zn-Ag-Ni appear to be reflecting the presence of a 0.4 m mineralized zone that has assays of 2.26% Zn, 0.21% Pb and 3.6 g/t Ag (DDH COP-98-1; Table 2). A magnetic low on line 14E is marked by the highest Zn response ratio (55) in the follow-up survey as well as a two sample Cu-Ni response. This multielement MMI anomaly is untested.

Table 1
Summary of significant mobile metal ion response ratios, follow-up survey.

Line	Element	Response Ratio
14E	Cu	35
	Zn	55
	Pb	9
	Co	25
	Ni	12
19E	Cu	46
	Zn	25
23E	Co	11
	Ni	7
	Ag	4.8
29E	Cu	40
	Pb	7
	Ag	4
	Co	4

The second anomalous MMI response tested by diamond drilling is marked by apical Zn-Cu-Pb-Ni and low Au responses that occur adjacent to a coincident airborne magnetic and ground EM anomaly on line 23. Diamond drilling of this multimedia anomaly (DDH COP-98-6; Table 2) did not intersect mineralization that would explain the geophysical and geochemical responses. The highest base metal assay was 1275 ppm Zn. A 0.7 m wide grey aphanitic "chert" (ultramylonite?) with 0.5-1% disseminated pyrite and traces of sphalerite and galena was intersected by this drill hole and this zone assayed 7.6 g/t Au and 90.6 g/t Ag.

Significant responses for Ag from north of the drill collar and a multisample Au response south of the drill collar on line 23E are untested.

DISCUSSION

Significant multisample, high contrast multielement geochemical signatures of a base- and precious-metal enriched mineralized zone are apparent in both the enzyme leach and mobile metal ion data collected from this survey. This result is somewhat surprising given the nature of the surficial deposits at Assean Lake. Thicknesses of up to 15 m of dense, grey glaciolacustrine clay mantling bedrock and up to 17 m of sand, gravel and boulders underlying the clay are documented. The mineralized zone is also concealed by 25 m of non-mineralized volcanic and sedimentary rocks. The severity of this type of overburden is witnessed by the abandoned exploration drill holes in this area.

Additionally, the recommended sampling procedure for the MMI surveys was modified by analyzing the -80 mesh size fraction of the B-horizon instead of collecting what is essentially a composite sample at each station. This was done to provide a basis for comparison between enzyme leach (-60 mesh) and MMI data (-80 mesh) from a particular soil horizon, albeit on different size fractions. The strong base metal geochemical signature of the main conductor at Assean Lake may, in part, be related to the location of the samples analysed by MMI. MMI base metal signatures are predicted to be sited at lower levels in the soil profile as compared to the location of precious metal responses, which should be developed between 10-30 cm below surface (Russell Birrell, pers. comm., 1998).

The ability of these techniques to provide meaningful data in this type of environment is significant since thick, lacustrine clay-dominated geological environments have traditionally been viewed as a serious impediment to the recognition of concealed mineralization using unconsolidated surficial geological materials (Smee, 1979, 1983).

Table 2.
Summary of assay intervals from diamond drill exploration conducted subsequent to follow-up MMI sample collection and interpretation.

Diamond Drill Hole	Line	Description
COP-98-1	14E,2+40N	0.4 m grading 2.26% Zn,
		0.21% Pb, 3.6 g/t Ag
COP-98-3	14E,5+20N	terminated
COP-98-5	14E, 2+15N	0.45 m grading 1% Zn and
		0.16% Pb
COP-98-4	7E,1+95N	260 ppb Au
COP-98-2	11E,1+50N	0.3 m grading 5% Zn,
		0.72% Pb, 16 g/t
		Ag 0.1 m grading 5% Zn,
		1.6% Pb, 9 g/t Ag
COP-98-6	23E,1+50N	0.3 m grading 22.2 g/t Au
		and 190 g/t Ag or 0.7 m grading
		7.6 g/t Au and 90.6 g/t Ag

Where signatures have been recognized there have been a plethora of attempts to explain the process by which the anomalies have been formed. Mechanisms such as electrochemical cells (Govett, 1972; Uthe, 1978) have been proposed, tested and locally demonstrated to be responsible for the development of surficial geochemical signatures attributed to buried mineralization (Govett, 1976; Govett and Atherden, 1987; Ferreira and Fedikow, 1990). Recently, the role of oxidizing groundwater and its access to mineralized zones with the subsequent development of a column of conductive groundwater transporting ions to surface has been assessed by studies in glaciated areas of thick overburden in northern Ontario (Jackson, 1995; Bajc, in prep., Stewart Hamilton, pers. comm.). The detection of geochemical anomalies from shallow and deep groundwater samples collected over concealed mineralization is suggestive of an upwardly mobile plume of metals generated by the interaction of oxidizing groundwater at its interface with mineralization or related alteration halo.

Numerous vapour-geochemical surveys, based on the collection of outcrop chip samples or fracture/shear zone/fault coatings, as well as studies utilizing passive vapour collection techniques (Fedikow and Amor, 1990; Klusman, 1993 and case histories therein), have demonstrated the presence of vapour-related geochemical anomalies overlying mineralized zones characterized by conspicuous metal (Hg and others) enrichment.

There are also a number of studies of vegetation geochemical signatures attributed to deeply buried mineral deposits premised on metal-enriched vapours and/or groundwaters transporting ions to surface where they are incorporated by vegetation root systems during nutrient acquisition. Fedikow and Dunn (1996) demonstrated a vegetation geochemical signature over the deeply buried (625 m) Hg-enriched Chisel North Zn-rich massive sulphide deposit. This deposit was discovered, in part, by the analysis of Hg contents in fracture coatings in outcrop near the surface projection of the deposit. Descriptions of the geological setting of the deposit (Galley et al., 1993) document the mobilization of metals from the deposit to adjacent wallrocks in response to post-depositional deformation and metamorphism. The observed metal-enrichment in vegetation growing over the deposit is attributed to the ascension of metal-enriched plumes and the subsequent uptake of metals via the vegetation root systems.

The abundance of geochemical case history studies relating to base- and precious-metal mineral exploration as well as hydrocarbon exploration (cf. Potter et al., 1996) indicate the vertical ascension of metals transported by a variety of carrier gases, that may be dissolved in groundwaters, is the preferred method for the development of surficial geochemical signatures from concealed sources. The possibility of isolating a solitary process responsible for these signatures would seem to be low given the fact that surficial geochemical signatures may be influenced by variabilities in the style of mineralization including environment of deposition and post-depositional overprinting (structures, protracted mineralization/alteration), attitude/geometry of the deposit, self-potential effects, accessibility by groundwater (oxidizing?), nature of surficial deposits and evapotranspiration. These factors and their roles in anomaly formation may not be consistent within a mineralized belt/ore district/grass roots exploration area and in fact can be demonstrated to be highly variable. Accordingly, rigid and quantified controls on anomaly formation at a well constrained sample site are not necessarily portable. This point is well demonstrated by the observed variability in surficial deposits at Assean Lake where exploratory drill holes encountered significant thicknesses in clays, sands, gravels and boulder alluvium over short distances. Conceivably, this variability may be the reason for subdued enzyme leach and mobile metal ion signatures over the flanking ground EM conductors.

The Assean Lake study also reveals some interesting variabilities between the elements contained within the mineralized zone and the anomalous elements in both MMI and enzyme leach data. Assay data indicate the mineralization to be enriched in Zn, Pb, Ag and Fe. High contrast anomalies for MMI Cu, Ni, Pd and Au and enzyme leach Cu and Ni are documented from the sampling transect in addition to the ore-related elements. Assays would most likely not have been done for Ni and Pd in this base metal exploration program, whereas Cu and Au assays accompanying the diamond drilling report are consistently nil for these metals. Explanations for this variance include unrecognized Cu and Au geochemical enrichments not reflected by the assay LLD or unrecognized zones of mineralization associated with the long strike length conductor. Regardless, the presence of associated pathfinder elements (of varying mobilities in the secondary environment) with ore-related elements can probably be considered a "bonus" in terms of isolating a geochemical response. In addition, the host rocks to the Assean Lake mineralized zone are part of the Thompson Nickel Belt where significant Ni-Cu orebodies are located and as such the presence of high background contents of these metals (including related Co and Pd) should not be unexpected either as associated elements in mineralized zones or as unique mineralized zones with this metal assemblage. The association of Au geochemical anomalies with the apparently Au "barren" nature of the Assean Lake mineralized zone is best explained by the presence of a separate gold mineralizing event at Assean Lake as represented by small but high grade Au occurrences. The shear-hosted vein type Dunbrack and Lindal Au deposits (up to 34 grams per

tonne Au over maximum widths of 1 m) occur due west of the study area along predominant east-trending structural features that characterize the Assean Lake area. This style of mineralization is clearly different from the submarine-massive sulphide type of deposit represented by the long strike length mineralized zone in the study area. The syn-depositional sulphide layer at Assean Lake was overprinted by later protracted deformational events, one of which was probably responsible for the formation of the Dunbrack and Lindal Au zones. It is therefore not unreasonable to expect some geochemical overprinting or redistribution of the mineralization. Interestingly, the MMI Au, Zn, Cd and Co anomalies are located at 600 m on the sampling transect directly over an inferred fault. Subsequent exploration on the Hunt property resulted in the discovery of a high-grade chert or ultramylonite-hosted zone of disseminated iron and base metal sulphides that assayed 22.2 g/t Au and 190 g/t Ag over 0.3 m or 0.7 m of 7.6 g/t Au and 90.6 g/t Ag. This would tend to substantiate the observed MMI Au and Ag responses as well as the potential for repetitions of Dunbrack and Lindal-type Au occurrences in the Assean Lake area. Additionally, an assay of 0.4% Cd obtained from a drill intersection during this same exploration phase indicates the presence of substantial associated Cd in the base metal mineralization, previously indicated by an anomalous MMI Cd signature in the original Hunt transect survey. The correspondence between mobile metal ion and enzyme leach geochemical responses and diamond drill results indicates that valuable exploration-supportive information can be derived by the analysis of B-horizon soil sample utilizing enzyme leach and mobile metal ion technologies. These techniques can be utilized at Assean Lake where current exploration has defined an area of base and precious metal potential previously underexplored because of the thickness and composition of the surficial deposits.

The need to assess the results of the Assean Lake enzyme leach and MMI study from a more tightly constrained perspective, including groundwater studies would be instructive so that the process of anomaly formation can be more clearly understood.

ACKNOWLEDGEMENTS

Doug Berk, Vio Varga, Gerry Benger, and Rick Unruh of the Geological Services Branch are thanked for sample preparation. Kelly Proutt is thanked for typing the manuscript. Bonnie Lenton is acknowledged for computer-aided drafting of the figures. Christine Kaszycki and Ric Syme are thanked for their constructive criticism of this report. Bob Clark (Activation Laboratories Ltd.) and Russell Birrell (Wamtech Pty. Ltd.) are thanked for their assistance with this project.

REFERENCES

Assessment File 93431
1985: Manitoba Energy & Mines, Minerals Division.

Bajc, A.F.
in prep.: A comparative analysis of enzyme leach and mobile metal ion selective extractions: case studies from glaciated terrain, northern Ontario; Ontario Geological Survey.

Birrell, R.
1996: MMI geochemistry: mapping the depths; Mining Magazine, v. 174, no. 5, p.306-307.

Clark, J.R.
1992: Detection of bedrock-related geochemical anomalies at the surface of transported overburden; Explore, v. 76, p.4-11.

Clark, J.R.
1993: Enzyme-induced leaching of B-horizon soils for mineral exploration in areas of glacial overburden; Trans. Instn. Min. Metall., (Sect. B: Appli. Earth Sci.), v. 102, p.B19-B29.

Fedikow, M.A.F. and Amor, S.D.
1990: Evaluation of a mercury-vapour detection system in base- and precious-metal exploration, northern Manitoba; J. Geochem. Explor., v. 38, no. 3, p.351-374.

Fedikow, M.A.F. and Dunn, C.E.
1996: The geochemistry of vegetation growing over the deeply buried Chisel North Zn-rich massive sulphide deposit, Snow Lake area; **in** EXTECH I: a multidisciplinary approach to massive sulphide research in the Rusty Lake-Snow Lake greenstone belts, Manitoba; (eds.) G.F. Bonham-Carter, A.G. Galley and G.E.M. Hall, Geological Survey of Canada, Bulletin 426, p.225-255.

Fedikow, M.A.F. and Ziehlke, D.V.
1996: Enzyme leach-based soil geochemical exploration for gold in deep overburden terranes, Assean Lake area, northeastern Manitoba; **in** Geological Association of Canada - Mineralogical Association of Canada Joint Annual Meeting, Winnipeg, Program with Abstracts, v. 21, p.A28.

Ferreira, K.J. and Fedikow, M.A.F.
1990: Specific conductance and hydrogen ion concentration as indicators of trace-element geochemical response in humus: Rod Cu-Zn and Big Island Zn-Cu-Au deposits, Manitoba (Canada); J. Geochem. Explor., v. 37, no. 2, p.185-203.

Galley, A.G., Bailes, A.H. and Kitzler, G.H.
1993: Geological setting and hydrothermal evolution of the Chisel Lake and North Chisel Zn-Pb-Cu-Ag-Au massive sulphide deposits, Snow Lake, Manitoba; Exploration and Mining Geology, v. 2, no. 4, p.271-295.

Gold, T. and Soter, S.
1980: The deep earth-gas hypothesis; Scientific American, v. 242, no. 6, p.154-165.

Govett, G.J.S.
1972: Differential secondary dispersion in transported soils and post-mineralization rocks: an electrochemical interpretation; **in** Geochemical Exploration 1972, Institute of Mining and Metallurgy, London, p.81-91.

Govett, G.J.S.
1976: Detection of deeply buried and blind sulphide deposits by measurement of H+ and conductivity of closely spaced surface soil samples; J. Geochem. Explor., v. 6, no. 3, p.359-382.

Govett, G.J.S. and Atherden, P.
1987: Electrogeochemical patterns in surface soils: detection of blind mineralization beneath exotic cover, Thalanga, Queensland, Australia; J. Geochem. Explor., v. 28, no. 1-3, p.201-218.

Haugh, I.
1969: Geology of the Split Lake area; Manitoba Department of Mines and Natural Resources, Mines Branch, Publication 65-2, 87p.

Jackson, R.G.
1995: The application of soil and water geochemistry to detect blind mineralization in areas of thick overburden; Ontario Geological Survey, Open File Report 5927, 151p.

Kaszycki, C.A.
1989: Surficial geology and till composition, northwestern Manitoba; Geological Survey of Canada, Open File 2118, 48p.

Klusman, R.W.
1993: Soil gas and related methods for natural resource exploration; Wiley and Sons, Toronto, 483p.

Malmqvist, L. and Kristiansson, K.
1984: Experimental evidence for an ascending microflow of geogas in the ground; Earth and Planetary Science Letters, v. 70, no. 2, p.407-416.

McRitchie, W.D.
1995: Mineral development potential in Manitoba - nickel in the southwest extension of the Thompson Nickel Belt; Manitoba Energy and Mines, Economic Geology Report ER95-2, 29p.

Potter II, R.W., Harrington, P.A., Silliman, A.H. and Viellenave, J.H.
1996: Significance of geochemical anomalies in hydrocarbon exploration; **in** Hydrocarbon migration and its near-surface expression; (eds.) D. Schumacher and M.A. Abrams, AAPG Memoir 66, p.431-439.

Smee, B.W.
1979: A theoretical estimation of ion mobilities through glaciolacustrine sediments: diffusion down a concentration gradient; **in** Current Research, Part A, Geological Survey of Canada, Paper 79-1A, p.367-374.

Smee, B.W.
1983: Laboratory and field evidence in support of the electrogeochemically enhanced migration of ions through glaciolacustrine sediment; J. Geochem. Explor., v. 19, no. 1-3, p.277-304.

Uthe, R.E.
1978: Assessment of soil conductance and pH in exploration geochemistry for selected mining areas of New Brunswick, Canada; unpublished Ph.D. thesis, University of New Brunswick, Fredericton, New Brunswick, 365p.

Wang, X., Cheng, Z., Lu,Y., Xu, L. and Xie, X.
1997: Nanoscale metals in Earth gas and mobile forms of metals in overburden in wide-spaced regional exploration for giant deposits in overburden terrains; J. Geochem. Explor., v. 58, no. 1, p.63-72.

Ziehlke, D.V.
1998: Report on drilling on the Hunt-14 claim (P2749F) at Assean Lake, Manitoba (NTS 64A/NW1); unpublished report, Strider Resources Limited

Appendix 1-1
Summary of analytical data for enzyme leach analysis
All values in parts per billion (ppb). A negative number indicates that analysis is below the limits of detection.

Sample	Metres	S.Q.Li	S.Q.Be	S.Q.Cl	S.Q.Sc	S.Q.Ti	V	Mn	Co	Ni	Cu	Zn
HUNT-1	**0**	18	-20	6043	32	-100	154	534	8	38	31	13
HUNT-2	**50**	87	-20	15609	39	-100	231	768	9	56	47	16
HUNT-3	**100**	40	-20	10657	34	-100	185	267	15	41	38	22
HUNT-4	**150**	94	-20	-3000	42	-100	243	1555	25	58	36	22
HUNT-5	**200**	54	-20	8586	42	116	672	874	17	65	40	43
HUNT-6	**250**	62	-20	15874	29	-100	247	698	8	55	35	11
HUNT-7	**300**	57	-20	-3000	30	-100	125	245	7	43	34	14
HUNT-8	**350**	77	-20	4584	45	-100	138	524	16	41	35	20
HUNT-9	**400**	43	-20	9772	53	-100	139	548	34	67	54	24
HUNT-10	**450**	30	-20	7687	49	-100	209	516	13	41	51	25
HUNT-11	**500**	155	-20	22741	108	235	310	1823	31	199	203	37
HUNT-12	**550**	103	-20	8825	62	-100	457	1025	18	68	133	40
HUNT-13	**600**	142	-20	6320	78	128	540	1132	44	87	80	66
HUNT-14	**650**	85	-20	-3000	48	-100	586	435	13	63	75	30
HUNT-15	**700**	29	-20	-3000	39	-100	141	210	6	35	28	24
HUNT-16	**750**	16	-20	6223	50	-100	135	289	9	37	31	22
HUNT-17	**800**	64	-20	4945	49	-100	124	544	13	54	37	17
HUNT-18	**850**	28	-20	7675	53	-100	213	172	7	30	32	16
HUNT-19	**900**	20	-20	4839	29	-100	464	1240	9	38	24	18
HUNT-20	**950**	28	-20	9024	28	-100	117	389	6	24	57	-10
HUNT-21	**1000**	32	-20	5093	59	-100	190	473	10	48	43	21
HUNT-22	**1050**	31	-20	21295	33	-100	148	800	10	28	68	15

Sample	Metres	Ga	Ge	As	Se	Br	Rb	Sr	Y	Zr	Nb	Mo
HUNT-1	**0**	2	1	17	85	223	19	289	31	74	2	16
HUNT-2	**50**	2	-1	19	-30	245	20	484	49	108	2	14
HUNT-3	**100**	1	-1	11	-30	357	20	443	16	66	3	10
HUNT-4	**150**	2	-1	15	-30	179	12	326	50	122	2	10
HUNT-5	**200**	5	1	18	-30	302	43	460	28	104	5	15
HUNT-6	**250**	1	-1	21	-30	227	19	638	37	100	2	8
HUNT-7	**300**	2	1	15	-30	201	17	295	40	143	2	5
HUNT-8	**350**	2	1	17	-30	195	22	376	50	273	4	4
HUNT-9	**400**	5	1	22	-30	262	39	427	59	207	4	4
HUNT-10	**450**	2	1	19	-30	295	15	330	69	172	2	5
HUNT-11	**500**	-1	2	25	-30	321	67	864	170	446	8	6
HUNT-12	**550**	3	1	17	69	81	43	747	68	160	4	6
HUNT-13	**600**	6	2	27	-30	322	81	671	51	501	7	2
HUNT-14	**650**	2	-1	21	-30	176	17	339	54	208	4	2
HUNT-15	**700**	2	-1	12	-30	204	17	376	46	195	2	3
HUNT-16	**750**	2	-1	11	-30	211	14	424	33	163	3	6
HUNT-17	**800**	2	-1	19	-30	182	22	347	50	279	2	4
HUNT-18	**850**	-1	-1	15	-30	237	16	319	38	127	2	4
HUNT-19	**900**	1	-1	12	-30	86	26	302	11	15	2	4
HUNT-20	**950**	1	-1	21	-30	229	22	449	24	51	1	8
HUNT-21	**1000**	2	1	17	-30	206	16	308	58	228	3	2
HUNT-22	**1050**	1	-1	20	-30	135	20	460	31	78	2	3

Appendix 1-1 Continued
Summary of analytical data for enzyme leach analysis
All values in parts per billion (ppb). A negative number indicates that analysis is below the limits of detection.

Sample	Metres	Ru	Rh	Pd	Ag	Cd	In	Sn	Sb	Te	I	Cs
HUNT-1	**0**	-1	-1	-1	-0.2	0.4	-0.2	-1	2	-1	97	-1
HUNT-2	**50**	-1	-1	-1	-0.2	0.4	-0.2	-1	1	-1	132	-1
HUNT-3	**100**	-1	-1	-1	-0.2	0.6	-0.2	1	1	1	141	-1
HUNT-4	**150**	-1	-1	-1	-0.2	-0.2	-0.2	-1	2	-1	163	-1
HUNT-5	**200**	-1	-1	-1	-0.2	0.4	-0.2	1	2	2	106	1
HUNT-6	**250**	-1	-1	-1	-0.2	0.4	-0.2	-1	2	1	149	-1
HUNT-7	**300**	-1	-1	-1	-0.2	-0.2	-0.2	1	1	-1	130	-1
HUNT-8	**350**	-1	-1	1	-0.2	-0.2	-0.2	-1	1	-1	90	-1
HUNT-9	**400**	-1	-1	-1	-0.2	0.7	-0.2	1	2	-1	80	-1
HUNT-10	**450**	-1	-1	-1	-0.2	-0.2	-0.2	1	2	-1	153	-1
HUNT-11	**500**	-1	-1	2	-0.2	0.7	-0.2	2	2	-1	93	2
HUNT-12	**550**	-1	-1	-1	-0.2	0.4	-0.2	-1	4	-1	15	-1
HUNT-13	**600**	-1	-1	-1	-0.2	1.1	-0.2	1	3	1	72	2
HUNT-14	**650**	-1	-1	-1	-0.2	-0.2	-0.2	-1	3	-1	62	-1
HUNT-15	**700**	-1	-1	-1	-0.2	-0.2	-0.2	-1	-1	-1	101	-1
HUNT-16	**750**	-1	-1	-1	-0.2	-0.2	-0.2	1	1	-1	96	-1
HUNT-17	**800**	-1	-1	-1	-0.2	-0.2	-0.2	1	2	-1	98	-1
HUNT-18	**850**	-1	-1	-1	-0.2	-0.2	-0.2	-1	1	-1	82	-1
HUNT-19	**900**	-1	-1	-1	-0.2	-0.2	-0.2	-1	1	-1	23	-1
HUNT-20	**950**	-1	-1	-1	-0.2	0.9	-0.2	2	-1	-1	60	-1
HUNT-21	**1000**	-1	-1	1	-0.2	-0.2	-0.2	-1	2	-1	142	-1
HUNT-22	**1050**	-1	-1	-1	-0.2	-0.2	-0.2	1	-1	-1	55	-1

Sample	Metres	Ba	La	Ce	Pr	Nd	Sm	Eu	Gd	Tb	Dy	Ho
HUNT-1	**0**	271	48	63	14	52	8	1	9	1	6	-1
HUNT-2	**50**	535	74	89	24	91	14	3	16	2	10	2
HUNT-3	**100**	325	26	65	8	27	4	-1	5	1	3	-1
HUNT-4	**150**	713	84	145	27	101	16	3	18	2	11	2
HUNT-5	**200**	626	47	98	15	52	7	2	10	1	6	1
HUNT-6	**250**	628	61	116	19	68	10	2	12	2	7	1
HUNT-7	**300**	298	57	84	18	67	10	2	12	2	8	1
HUNT-8	**350**	549	67	148	23	86	14	3	18	2	11	2
HUNT-9	**400**	338	97	238	32	113	17	3	21	3	14	2
HUNT-10	**450**	486	99	125	31	121	18	4	22	3	15	3
HUNT-11	**500**	1041	292	578	80	310	46	9	54	6	36	7
HUNT-12	**550**	1514	80	195	30	122	23	5	25	3	15	3
HUNT-13	**600**	763	69	158	22	87	14	3	15	2	11	2
HUNT-14	**650**	799	80	150	26	102	15	3	19	2	13	2
HUNT-15	**700**	388	65	130	20	75	12	2	16	2	10	2
HUNT-16	**750**	489	51	99	16	58	9	2	10	1	8	1
HUNT-17	**800**	459	63	123	21	85	13	3	17	2	12	3
HUNT-18	**850**	401	51	101	18	64	9	2	12	2	9	2
HUNT-19	**900**	261	16	34	5	19	2	-1	3	-1	2	-1
HUNT-20	**950**	249	34	48	10	38	5	-1	6	1	5	1
HUNT-21	**1000**	500	71	128	24	96	15	3	17	3	13	3
HUNT-22	**1050**	395	51	102	16	55	8	2	10	1	7	1

Appendix 1-1 Continued
Summary of analytical data for enzyme leach analysis

All values in parts per billion (ppb). A negative number indicates that analysis is below the limits of detection.

Sample	Metres	Er	Tm	Yb	Lu	Hf	Ta	W	Re	Os	Ir	Pt
HUNT-1	**0**	3	-1	3	-1	2	-1	-1	-0.1	-1	-1	-1
HUNT-2	**50**	4	-1	5	1	3	-1	1	-0.1	-1	-1	-1
HUNT-3	**100**	1	-1	2	-1	1	-1	-1	-0.1	-1	-1	-1
HUNT-4	**150**	4	-1	5	1	3	-1	-1	-0.1	-1	-1	-1
HUNT-5	**200**	3	-1	3	-1	3	-1	2	-0.1	-1	-1	-1
HUNT-6	**250**	3	-1	3	-1	2	-1	1	-0.1	-1	-1	-1
HUNT-7	**300**	3	-1	4	-1	4	-1	-1	-0.1	-1	-1	-1
HUNT-8	**350**	5	-1	6	1	7	-1	-1	-0.1	-1	-1	-1
HUNT-9	**400**	6	-1	6	1	6	-1	-1	-0.1	-1	-1	-1
HUNT-10	**450**	6	-1	7	1	4	-1	-1	-0.1	-1	-1	-1
HUNT-11	**500**	14	2	14	2	10	2	1	-0.1	-1	-1	-1
HUNT-12	**550**	6	1	7	1	3	-1	-1	-0.1	-1	-1	-1
HUNT-13	**600**	5	-1	6	1	13	-1	1	-0.1	-1	-1	-1
HUNT-14	**650**	5	-1	6	1	5	-1	-1	-0.1	-1	-1	-1
HUNT-15	**700**	4	-1	4	-1	6	-1	-1	-0.1	-1	-1	-1
HUNT-16	**750**	3	-1	4	-1	4	-1	-1	-0.1	-1	-1	-1
HUNT-17	**800**	5	-1	6	1	8	-1	-1	-0.1	-1	-1	-1
HUNT-18	**850**	4	-1	4	-1	4	-1	-1	-0.1	-1	-1	-1
HUNT-19	**900**	-1	-1	-1	-1	-1	-1	-1	-0.1	-1	-1	-1
HUNT-20	**950**	2	-1	2	-1	-1	-1	-1	-0.1	-1	-1	-1
HUNT-21	**1000**	5	-1	6	-1	6	-1	-1	-0.1	-1	-1	-1
HUNT-22	**1050**	3	-1	3	-1	1	-1	-1	-0.1	-1	-1	-1

Sample	Metres	Au	S.Q.Hg	Tl	Pb	Bi	Th	U
HUNT-1	**0**	-0.1	-1	-1	8	-1	8	2
HUNT-2	**50**	-0.1	-1	-1	8	-1	21	2
HUNT-3	**100**	-0.1	-1	-1	7	-1	15	3
HUNT-4	**150**	-0.1	-1	-1	10	-1	29	2
HUNT-5	**200**	-0.1	-1	-1	12	-1	34	6
HUNT-6	**250**	-0.1	-1	-1	5	-1	32	2
HUNT-7	**300**	-0.1	-1	-1	9	-1	25	3
HUNT-8	**350**	-0.1	-1	-1	10	-1	46	4
HUNT-9	**400**	-0.1	-1	-1	7	-1	41	6
HUNT-10	**450**	-0.1	-1	-1	9	-1	30	3
HUNT-11	**500**	-0.1	-1	-1	23	-1	120	7
HUNT-12	**550**	-0.1	-1	-1	21	-1	43	5
HUNT-13	**600**	-0.1	-1	-1	18	-1	88	27
HUNT-14	**650**	-0.1	-1	-1	15	-1	45	5
HUNT-15	**700**	-0.1	-1	-1	7	-1	34	6
HUNT-16	**750**	-0.1	-1	-1	7	-1	29	8
HUNT-17	**800**	-0.1	-1	-1	10	-1	45	5
HUNT-18	**850**	-0.1	-1	-1	10	-1	28	3
HUNT-19	**900**	-0.1	-1	-1	5	-1	6	1
HUNT-20	**950**	-0.1	-1	-1	5	-1	13	-1
HUNT-21	**1000**	-0.1	-1	-1	8	-1	38	3
HUNT-22	**1050**	-0.1	-1	-1	7	-1	23	1

Appendix 1-2
Summary of enzyme leach analytical data for field duplicate sample pairs
All data in parts per billion (ppb). A negative number indicates that analysis is below the limits of detection.

Sample ID:	S.Q.Li	S.Q.Be	S.Q.Cl	S.Q.Sc	S.Q.Ti	V	Mn	Co	Ni	Cu	Zn	Ga
HUNT-10d1	30	-20	7687	49	-100	209	516	13	41	51	25	2
HUNT-21d1	32	-20	5093	59	-100	190	473	10	48	43	21	2
HUNT-20d2	28	-20	9024	28	-100	117	389	6	24	57	-10	1
HUNT-22d2	31	-20	21295	33	-100	148	800	10	28	68	15	1

Sample ID:	Ge	As	Se	Br	Rb	Sr	Y	Zr	Nb	Mo	Ru	Rh
HUNT-10d1	1	19	-30	295	15	330	69	172	2	5	-1	-1
HUNT-21d1	1	17	-30	206	16	308	58	228	3	2	-1	-1
HUNT-20d2	-1	21	-30	229	22	449	24	51	1	8	-1	-1
HUNT-22d2	-1	20	-30	135	20	460	31	78	2	3	-1	-1

Sample ID:	Pd	Ag	Cd	In	Sn	Sb	Te	I	Cs	Ba	La	Ce
HUNT-10d1	-1	-0.2	-0.2	-0.2	1	2	-1	153	-1	486	99	125
HUNT-21d1	1	-0.2	-0.2	-0.2	-1	2	-1	142	-1	500	71	128
HUNT-20d2	-1	-0.2	0.9	-0.2	2	-1	-1	60	-1	249	34	48
HUNT-22d2	-1	-0.2	-0.2	-0.2	1	-1	-1	55	-1	395	51	102

Sample ID:	Pr	Nd	Sm	Eu	Gd	Tb	Dy	Ho	Er	Tm	Yb	Lu	Hf
HUNT-10d1	31	121	18	4	22	3	15	3	6	-1	7	1	4
HUNT-21d1	24	96	15	3	17	3	13	3	5	-1	6	-1	6
HUNT-20d2	10	38	5	-1	6	1	5	1	2	-1	2	-1	-1
HUNT-22d2	16	55	8	2	10	1	7	1	3	-1	3	-1	1

Sample ID:	Ta	W	Re	Os	Ir	Pt	Au	S.Q.Hg	Tl	Pb	Bi	Th	U
HUNT-10d1	-1	-1	-0.1	-1	-1	-1	-0.1	-1	-1	9	-1	30	3
HUNT-21d1	-1	-1	-0.1	-1	-1	-1	-0.1	-1	-1	8	-1	38	3
HUNT-20d2	-1	-1	-0.1	-1	-1	-1	-0.1	-1	-1	5	-1	13	-1
HUNT-22d2	-1	-1	-0.1	-1	-1	-1	-0.1	-1	-1	7	-1	23	1

Appendix 2
Emzyme leach profiles, Hunt transect

Cu (ppb)

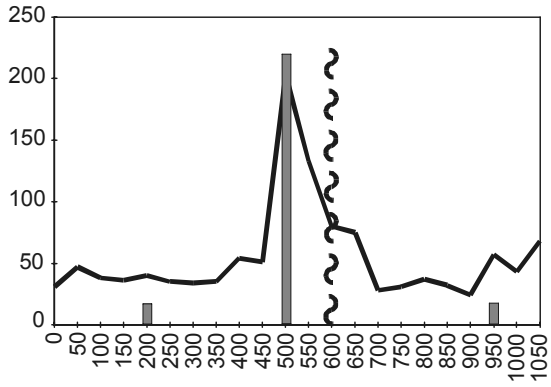

Pb (ppb)

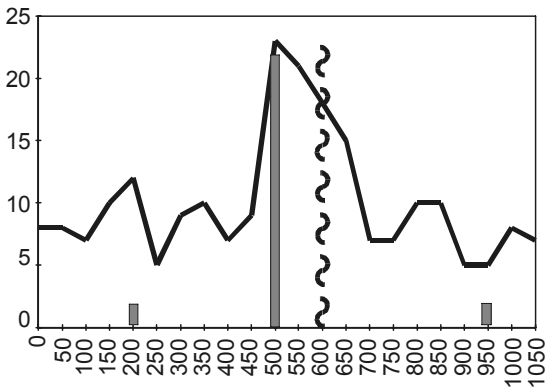

Zn (ppb)

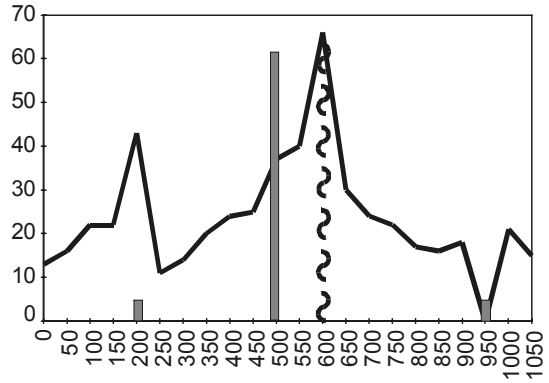

Ni (ppb)

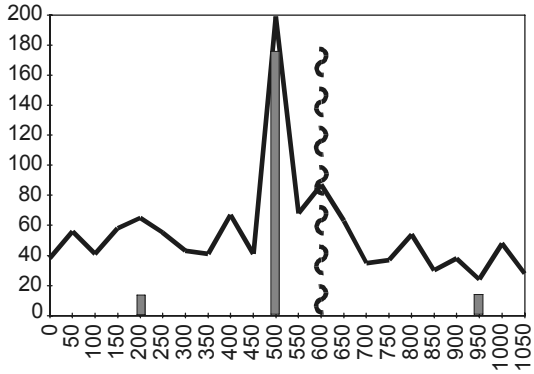

Co (ppb)

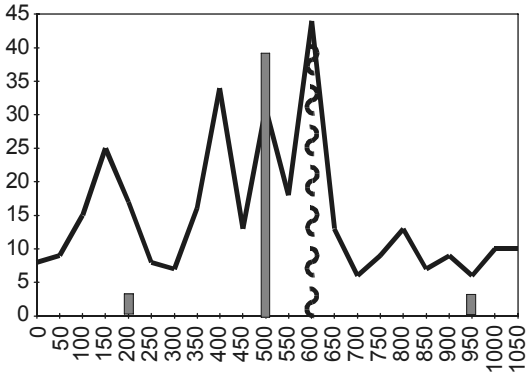

Metres Along Hunt Transect Looking East

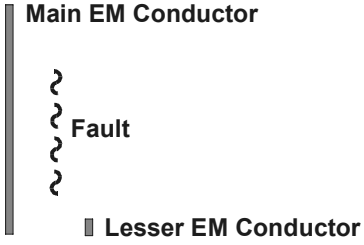

Appendix 2 Continued
Emzyme leach profiles, Hunt transect

As (ppb)

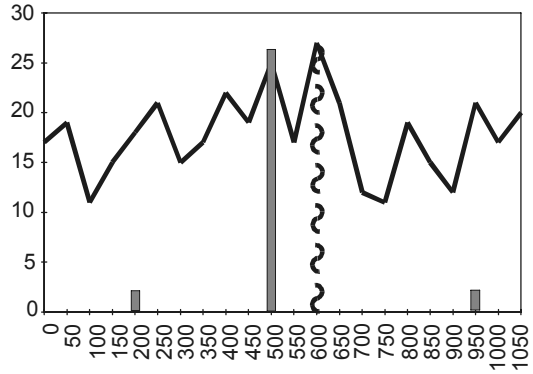

La (ppb)

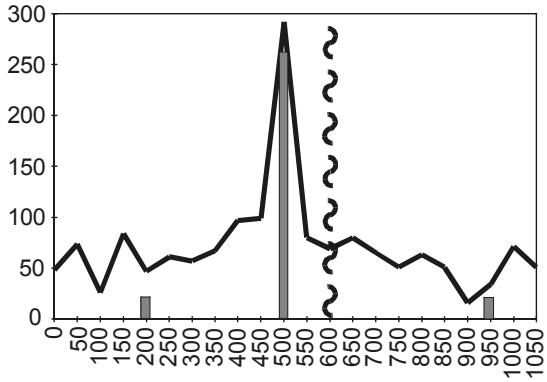

Ce (ppb)

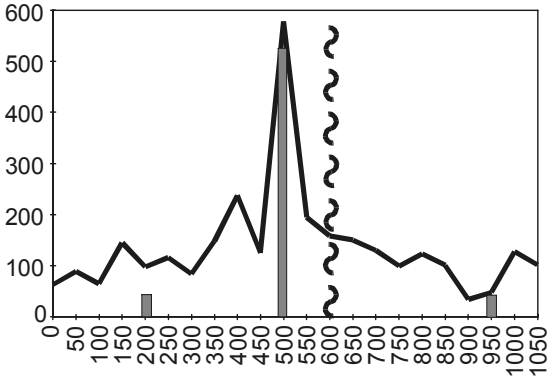

Pr (ppb)

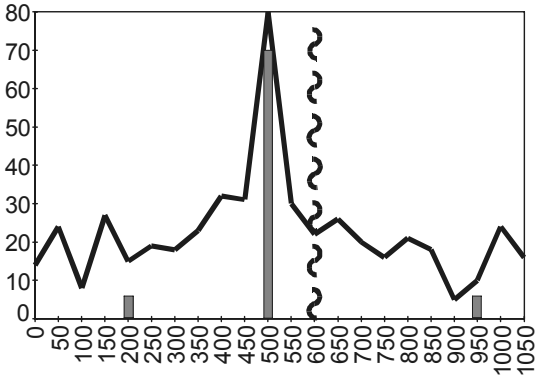

Nd (ppb)

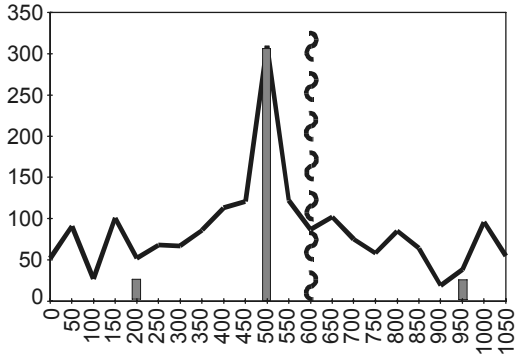

Metres Along Hunt Transect Looking East

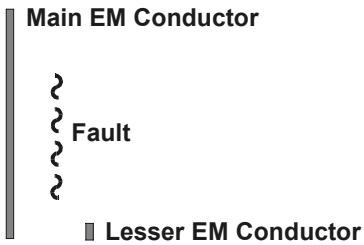

Appendix 2 Continued
Emzyme leach profiles, Hunt transect

Sm (ppb)

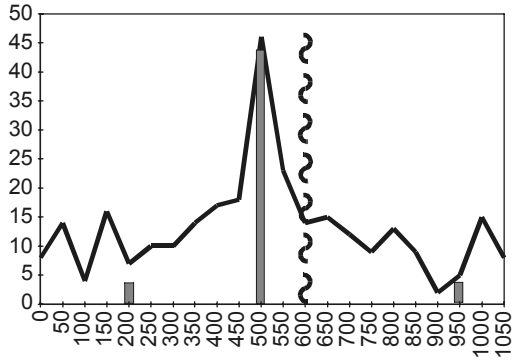

Eu (ppb)

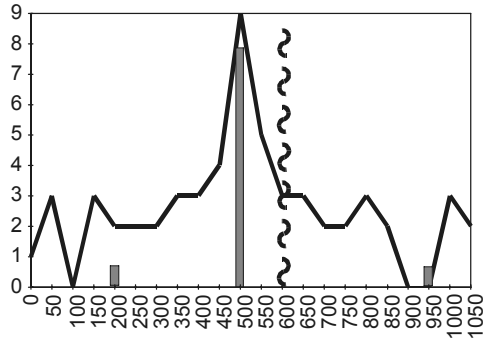

Gd (ppb)

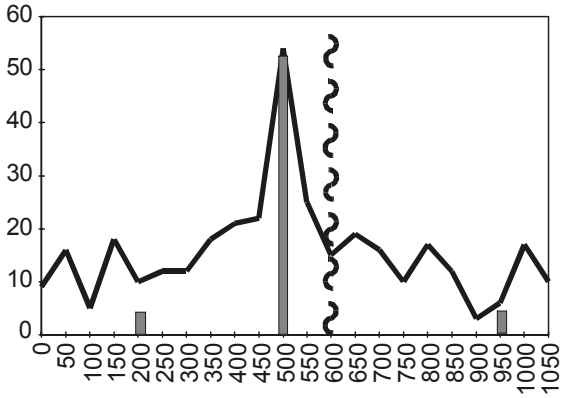

Tb (ppb)

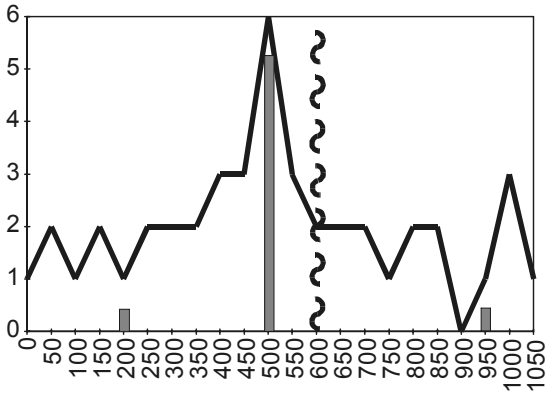

Dy (ppb)

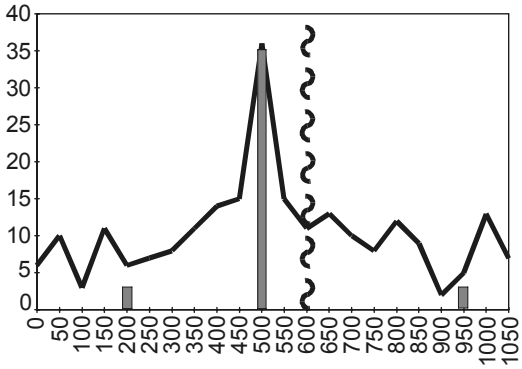

Metres Along Hunt Transect Looking East

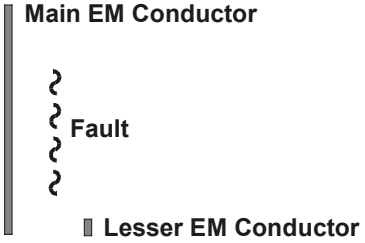

Appendix 2 Continued
Emzyme leach profiles, Hunt transect

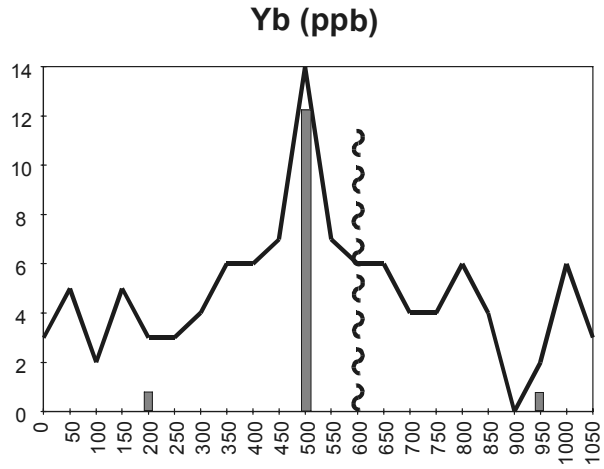

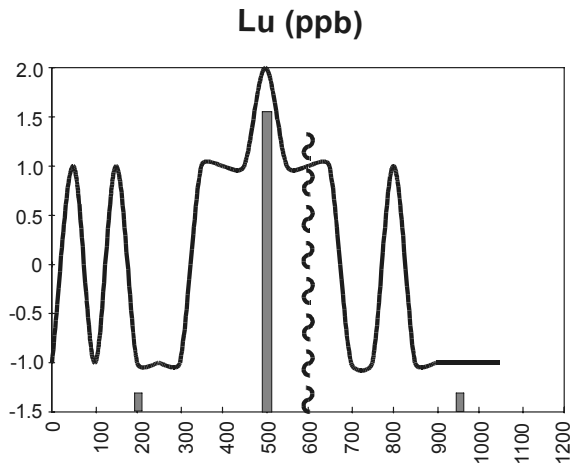

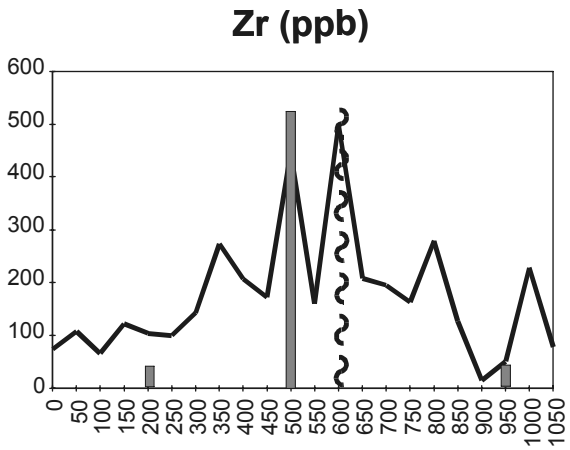

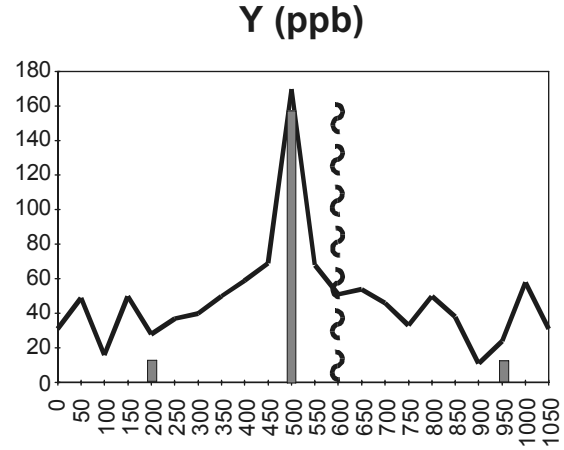

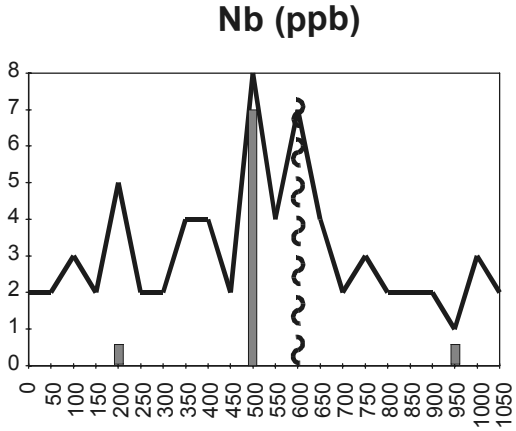

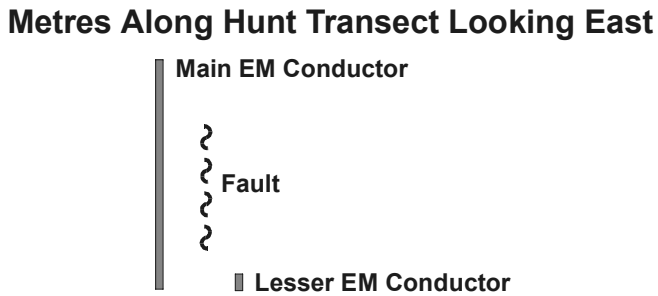

Appendix 2 Continued
Emzyme leach profiles, Hunt transect

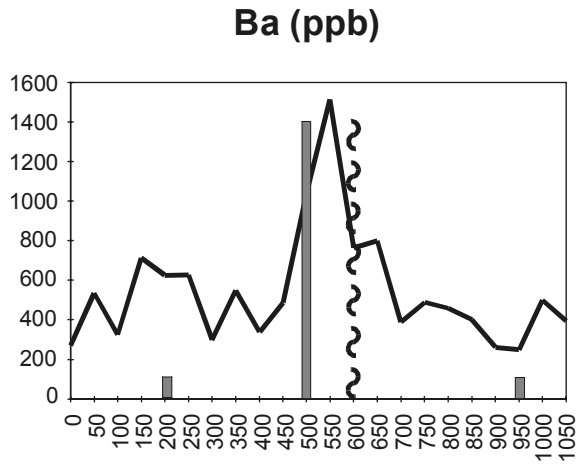

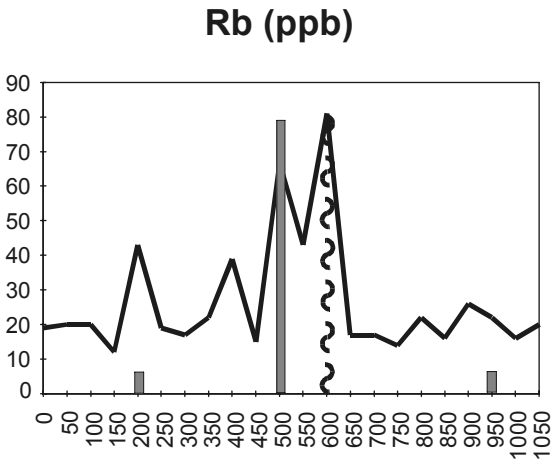

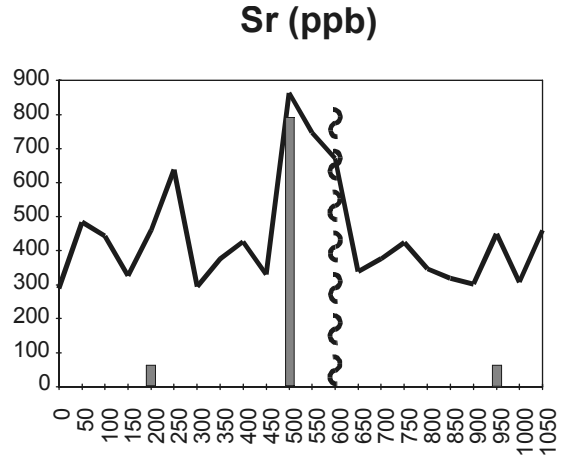

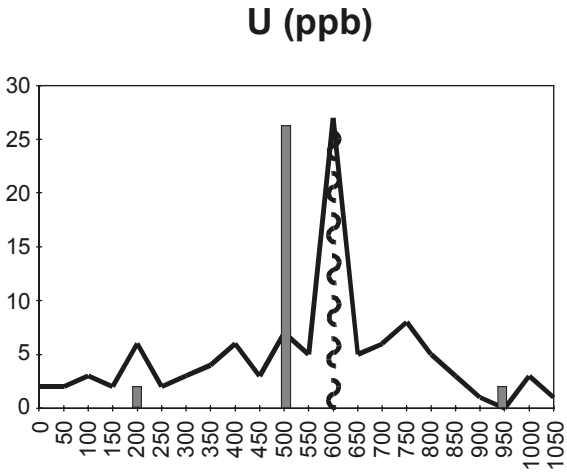

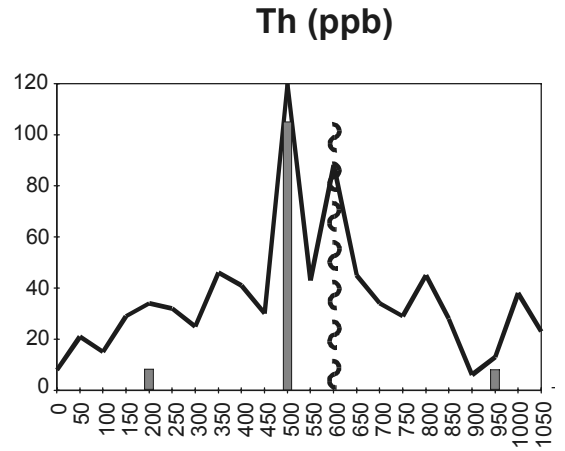

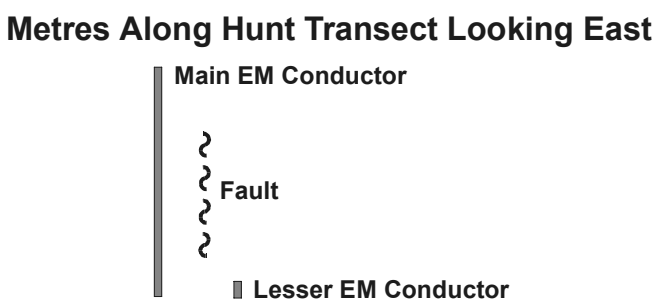

Appendix 2 Continued
Emzyme leach profiles, Hunt transect

Pd (ppb)

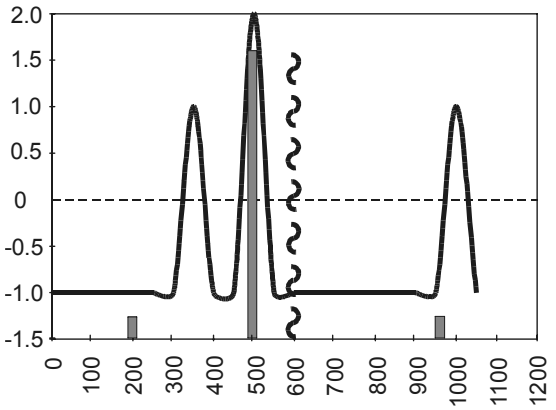

Mo (ppb)

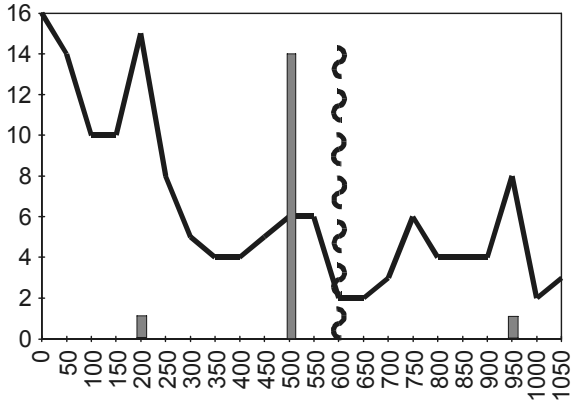

Se (ppb)

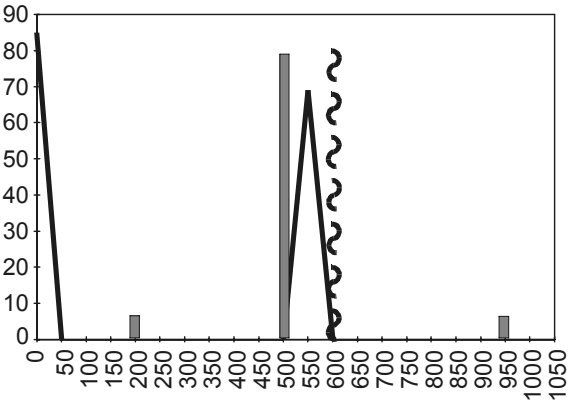

Te (ppb)

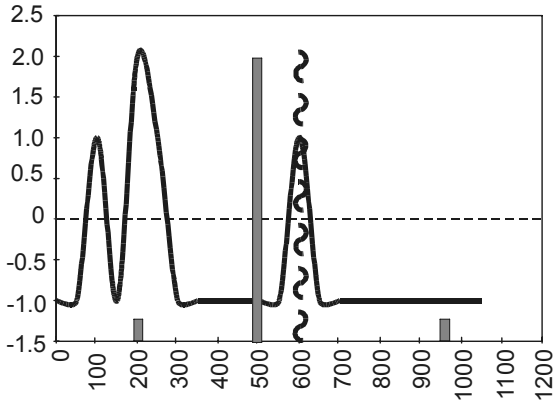

Br (ppb)

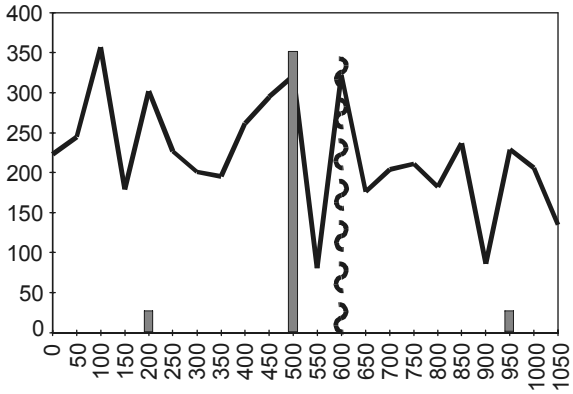

Metres Along Hunt Transect Looking East

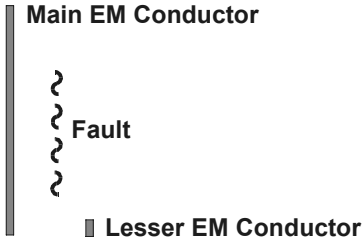

Appendix 2 Continued
Emzyme leach profiles, Hunt transect

I (ppb)

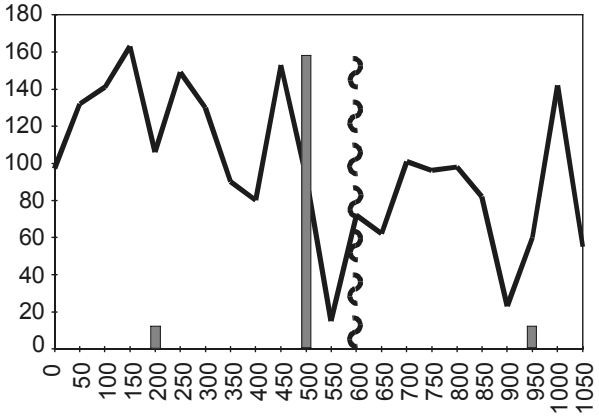

SQLI (ppb)

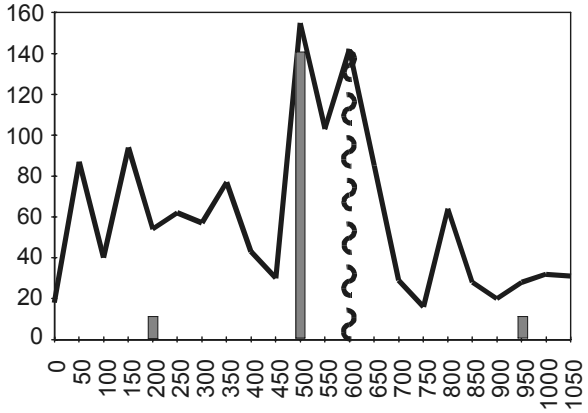

SQSc (ppb)

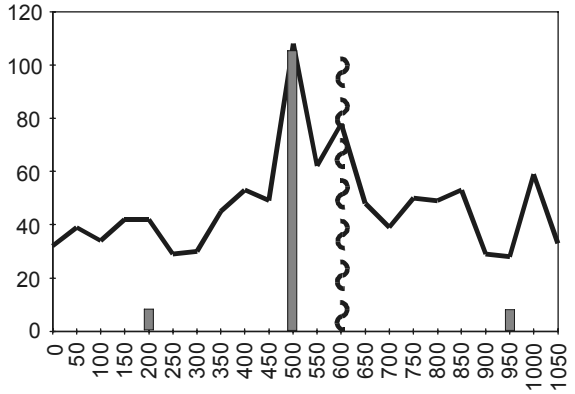

Ta (ppb)

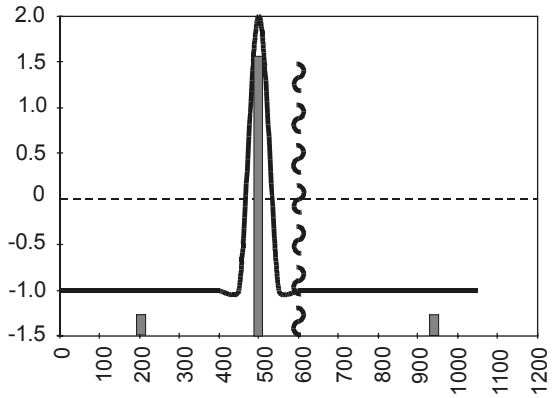

W (ppb)

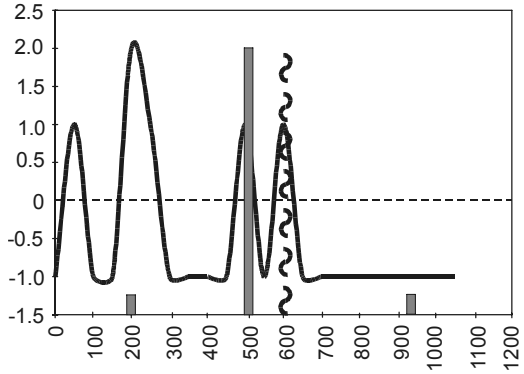

Metres Along Hunt Transect Looking East

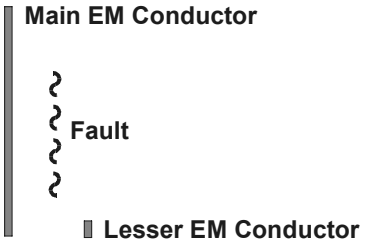

Appendix 2 Continued
Emzyme leach profiles, Hunt transect

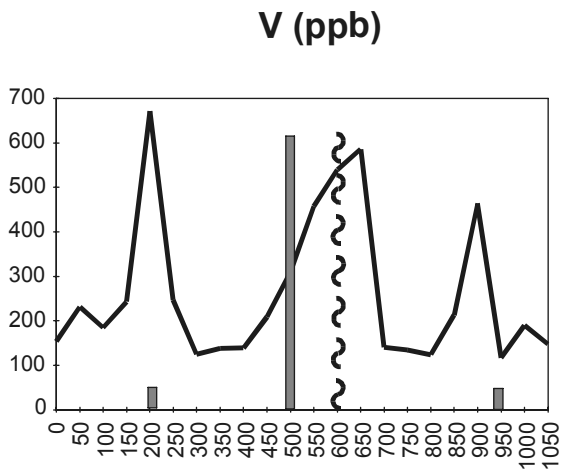

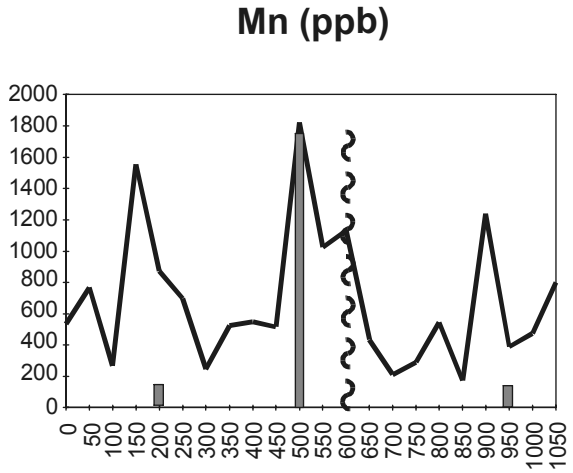

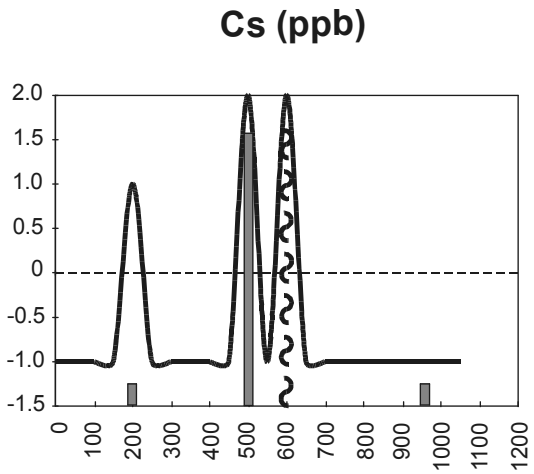

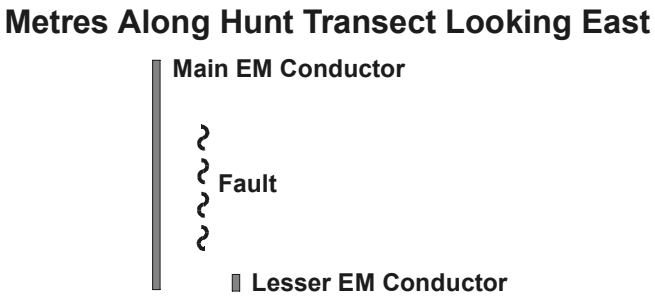

Appendix 3
Mobile metal ion analytical data for Hunt transect samples including field and analytical duplicates

Sample	Metres	Cu	Pb	Zn	Ni	Cd	Au	Ag	Co	Pd
Hunt-1	0	47	90	18	508	22	<1	14	22	<1
Hunt-2	50	98	118	<5	411	19	2	31	12	<1
Hunt-3	100	<5	83	127	54	10	<1	2	17	<1
Hunt-4	150	135	205	<5	617	15	1	37	68	<1
Hunt-5	200	<5	83	<5	740	<10	<1	14	18	<1
Hunt-6	250	<5	68	<5	659	10	1	25	15	<1
Hunt-7	300	<5	135	<5	444	<10	<1	13	<10	<1
Hunt-8	350	<5	154	63	392	<10	<1	9	<10	<1
Hunt-9	400	<5	53	33	341	11	<1	8	25	<1
Hunt-10	450	36	110	<5	509	<10	<1	10	25	<1
Hunt-11	500	131	125	<5	1300	25	1	28	79	<1
Hunt-12	550	1240	161	64	416	28	1	74	45	<1
Hunt-13	600	22	44	236	<10	30	37	20	129	53
Hunt-14	650	87	203	<5	1910	<10	<1	35	12	<1
Hunt-15	700	<5	134	23	622	<10	<1	14	<10	<1
Hunt-16	750	<5	64	<5	471	<10	<1	13	<10	<1
Hunt-17	800	<5	104	<5	445	<10	<1	10	18	<1
Hunt-18	850	<5	139	<5	377	<10	<1	9	16	<1
Hunt-19	900	24	128	<5	1100	10	<1	16	91	<1
Hunt-20	950	<5	34	<5	304	<10	<1	13	17	<1
Hunt-21	1000	63	192	<5	726	<10	1	17	19	<1
Hunt-22	1050	<5	166	<5	159	13	1	9	12	<1

Hunt transect MMI analytical data. All values in parts per billion (ppb).

Sample	Metres	Cu	Pb	Zn	Ni	Cd	Au	Ag	Co	Pd
Mobile Metal Ion Field Duplicates										
Hunt-10d1	450	36	110	<5	509	<10	<1	10	25	<1
Hunt-23d1	450	13	106	66	693	12	<1	14	17	<1
Hunt-19d2	900	24	128	<5	1100	10	<1	16	91	<1
Hunt-24d2	900	41	20	53	1050	76	<1	14	119	<1
Mobile Metal Ion Analytical Duplicates										
Hunt-1	0 m	47	90	18	508	22	<1	14	22	<1
Hunt-1d	0 m	63	126	23	541	27	<1	15	19	<1
Hunt-13	600 m	22	44	236	<10	30	37	20	129	53
Hunt-13d	600 m	30	84	251	<10	33	40	21	133	55

Field and analytical mobile metal ion duplicate sample data. All values in parts per billion (ppb).

Appendix 4
Mobile metal ion profiles and response ratios, Hunt transect

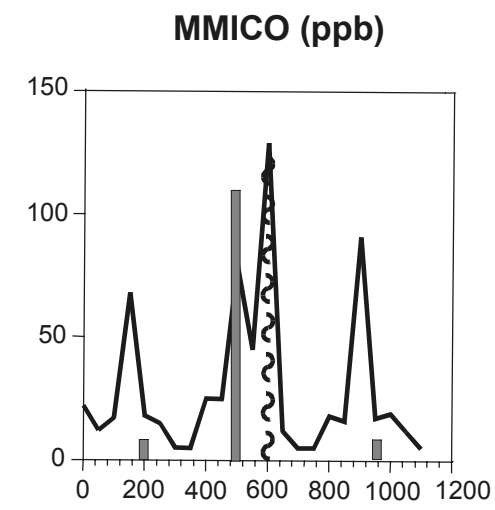

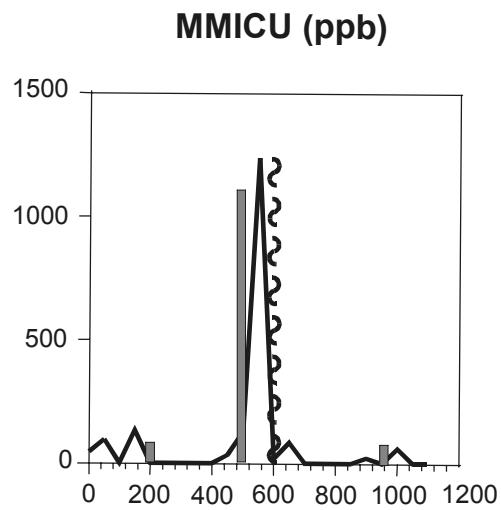

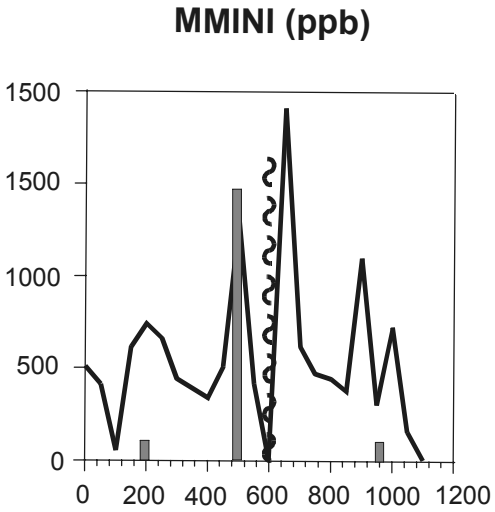

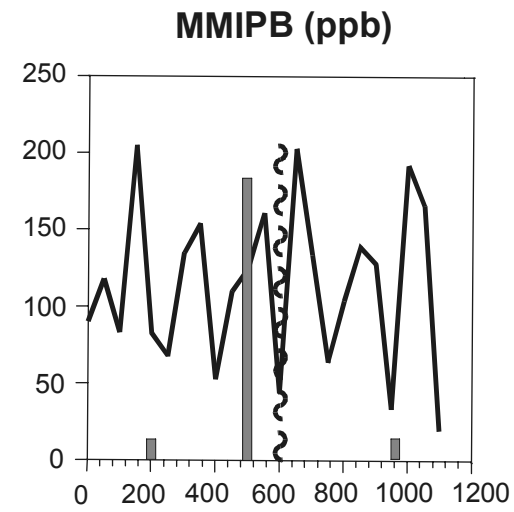

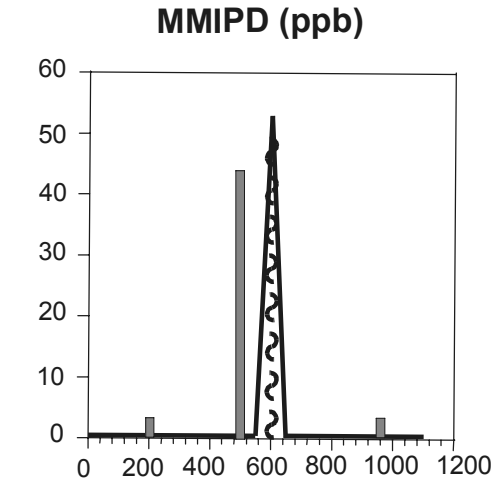

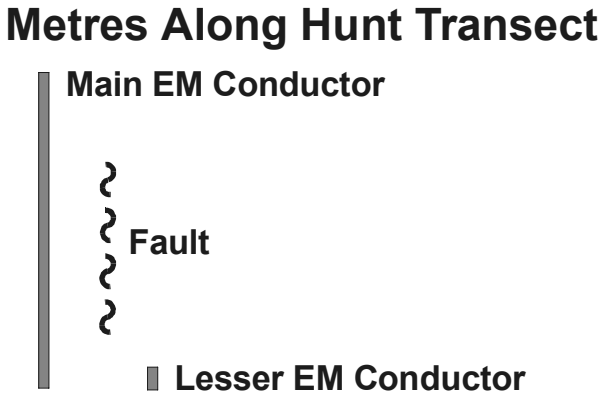

Appendix 4 Continued
Mobile metal ion profiles and response ratios, Hunt transect

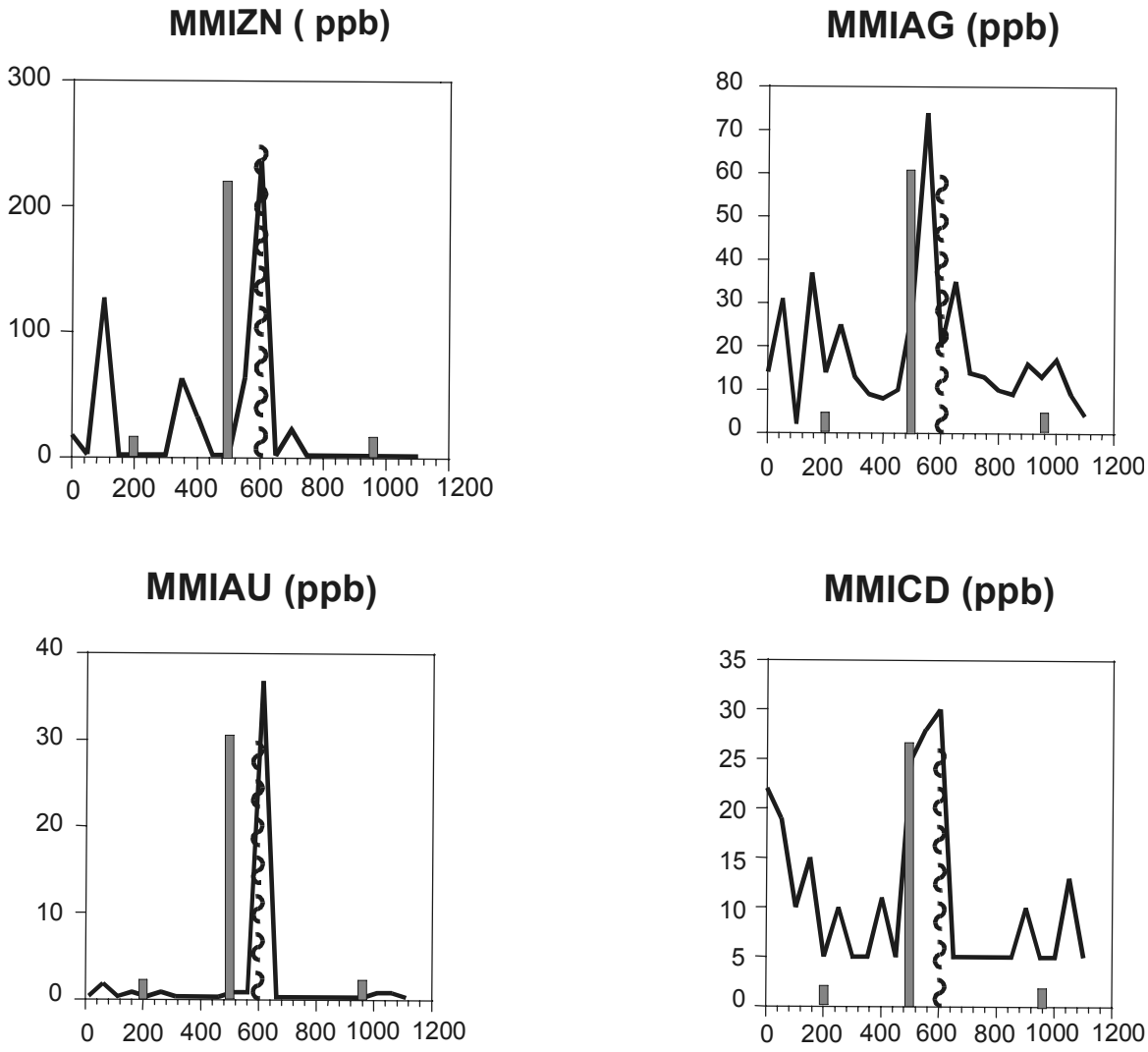

Appendix 5
Analytical data (ppb) for mobile metal ion analyses, follow-up survey, Hunt claims

Sample	Line	Cu	Zn	Pb	Au	Co	Ni	Ag
1	**8E,1+00N**	6	124	28	0.125	113	305	5.77
2	**7E,1+25N**	9	2.5	10	0.31	5	205	16.1
3	**14E,1+50N**	156	2.5	10	0.31	5	154	8.91
4	**14E,1+75N**	117	19	10	0.125	3	148	9.58
5	**14E,2N**	167	71	10	0.28	15	496	21.4
6	**14E,2+25N**	199	82	21	0.32	7	246	16.5
7	**14E,2+50N**	13	11	10	0.125	52	182	3.03
8	**14E,2+75N**	379	145	92	0.125	11	519	19.3
9	**14E,3N**	151	27	10	0.27	4	88	16.4
10	**14E,3+25N**	158	83	20	0.125	15	229	16.3
11	**14E,3+50N**	16	2.5	10	0.38	5	83	18.1
12	**14E,3+75N**	119	141	10	0.26	6	411	19.3
13	**14E,4N**	248	113	47	0.28	9	301	11.3
14	**14E,4+25N**	235	40	10	0.38	1	193	26
15	**14E,4+50N**	28	2.5	10	0.36	1	56	8.14
16	**14E,4+75N**	9	2.5	10	0.31	1	96	8.38
17	**14E,5N**	25	9	10	0.33	2	109	9.02
18	**14E,5+21N**	20	19	10	0.26	5	93	11.1
19	**14E,5+50N**	45	18	10	0.125	4	124	12.5
20	**14E,6+50N**	10	7	10	0.125	6	145	8.69
21	**14E,6+50N**	9	5	10	0.28	6	193	13.7
22	**14E,6+75N**	110	84	10	0.125	21	467	7.63
23	**14E,7N**	17	2.5	10	0.29	2	105	7.95
24	**14E,7+25N**	101	2.5	31	0.125	2	122	9.32
25	**14E,7+50N**	63	2.5	10	0.27	2	46	4.86
26	**14E,7+75N**	293	87	10	0.125	7	520	17.5
27	**19E,1+50N**	9	2.5	10	0.35	2	70	10.8
28	**19E,1+75N**	19	6	10	0.39	2	63	7.58
29	**19E,2N**	21	2.5	10	0.28	2	53	9.8
30	**19E,2+25N**	51	2.5	29	0.31	1	36	3.93
31	**19E,2+25N**	57	6	10	0.45	0.5	30	2.74
32	**19E,2+50N**	17	2.5	10	0.32	1	34	3.59
33	**19E,2+75N**	14	2.5	10	0.3	5	94	6.46
34	**19E,3N**	19	2.5	10	0.125	4	83	3.93
35	**19E,3+25N**	506	64	40	0.125	2	108	9.69
36	**23E,1+25N**	8	2.5	10	0.37	2	108	16
37	**23E,1+43N**	62	2.5	10	0.28	0.5	40	3.7
38	**23E,1+81N**	2.5	8	10	0.125	3	321	12
39	**23E,2N**	208	29	23	0.35	3	119	12.1
40	**23E,2+28N**	106	31	10	0.125	4	88	20.2
41	**23E,2+58N**	51	7	10	0.125	4	25	15.6
42	**23E,2+80N**	68	6	10	0.125	5	42	22.4
43	**23E,3N**	299	13	10	0.125	21	76	24.9
44	**23E,1N**	10	2.5	10	0.28	2	71	7.97
45	**29E,0+50N**	258	125	10	0.26	4	422	16.2
46	**29E,0+75N**	220	66	10	0.125	8	554	19
47	**29E,1N**	146	8	10	0.4	3	133	16.7
48	**29E,1+25N**	17	5	10	0.33	2	49	10.1
49	**29E,1+50N**	97	112	10	0.3	2	169	8.79
50	**29E,1+75N**	158	37	10	0.28	5	358	15.9
51	**29E,2N**	441	91	68	0.125	4	129	19.8
52	**29E,2N**	171	10	10	0.125	2	39	15.3

Appendix 6
Field and analytical duplicates (ppb) for mobile metal ion follow-up surveys, Hunt claims, Assean Lake

Field Duplicates								
Sample	**Line**	**Cu**	**Zn**	**Pb**	**Au**	**Co**	**Ni**	**Ag**
20	14E,6+50N	10	7	10	<0.25	6	145	8.69
21	14E,6+50N	9	5	10	0.28	6	193	13.7
51	29E,2N	441	91	68	<0.25	4	129	19.8
52	29E,2N	171	10	10	<0.25	2	39	15.3

Analytical Duplicates								
Sample	**Line**	**Cu**	**Zn**	**Pb**	**Au**	**Co**	**Ni**	**Ag**
1	8E,1+00N	6	124	28	<0.25	113	305	5.77
1	8E,1+00N	5	115	38	<0.25	102	308	5.86
13	14E,4N	248	113	47	0.28	9	301	11.3
13	14E,4N	223	99	<20	0.25	11	294	9.83
25	14E,7+50N	63	2.5	<20	0.27	2	46	4.86
25	14E,7+50N	65	7	<20	0.3	2	44	4.75
37	23E,1+43N	62	2.5	<20	0.28	<1	40	3.7
37	23E,1+43N	59	<5	<20	0.26	<1	46	4.22
49	29E,1+50N	97	112	<20	0.3	2	169	8.79
49	29E,1+50N	98	170	<20	0.3	3	172	8.83

Appendix 7
Hunt Transect MMI Response Ratios

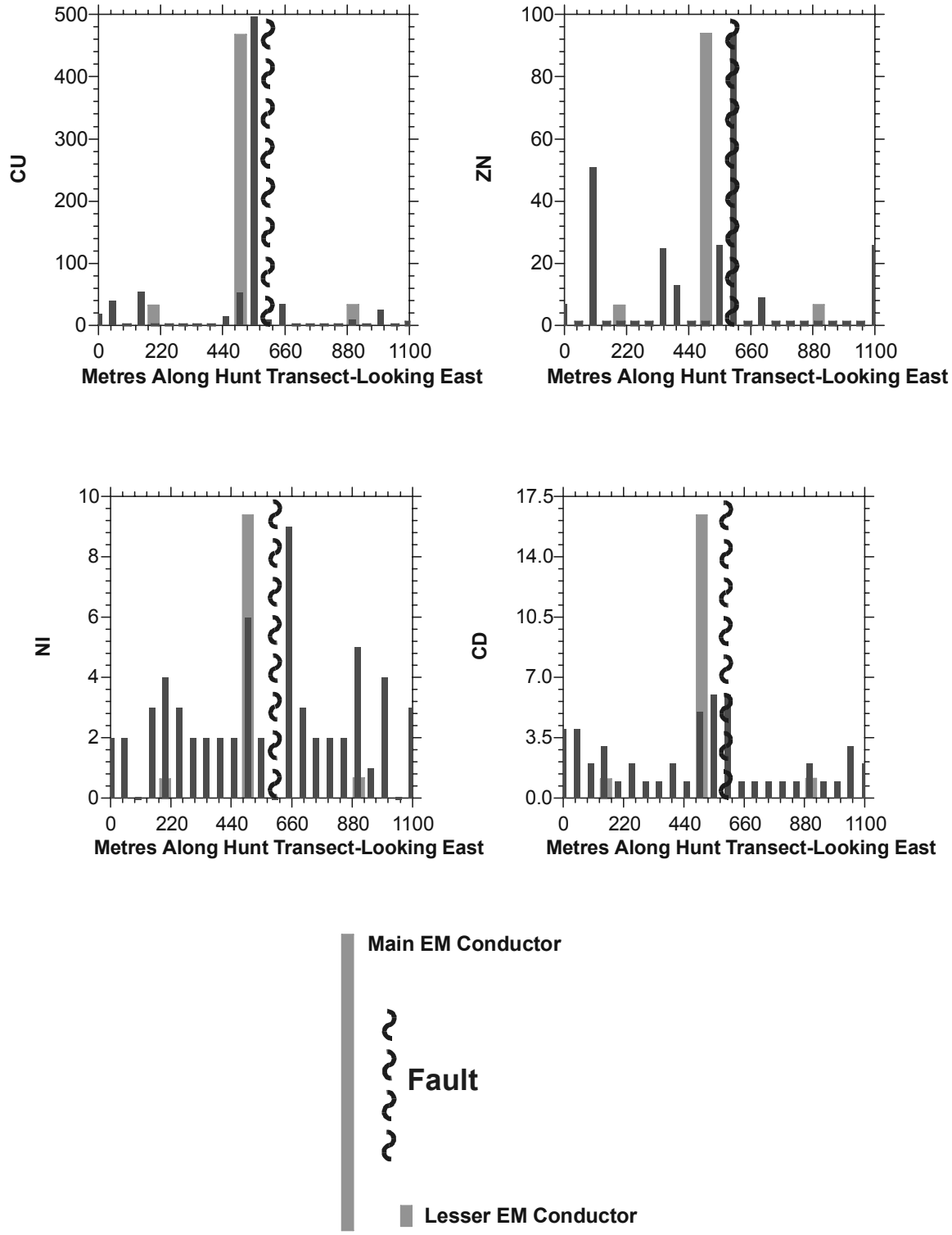

Appendix 7 Continued
Hunt Transect MMI Response Ratios

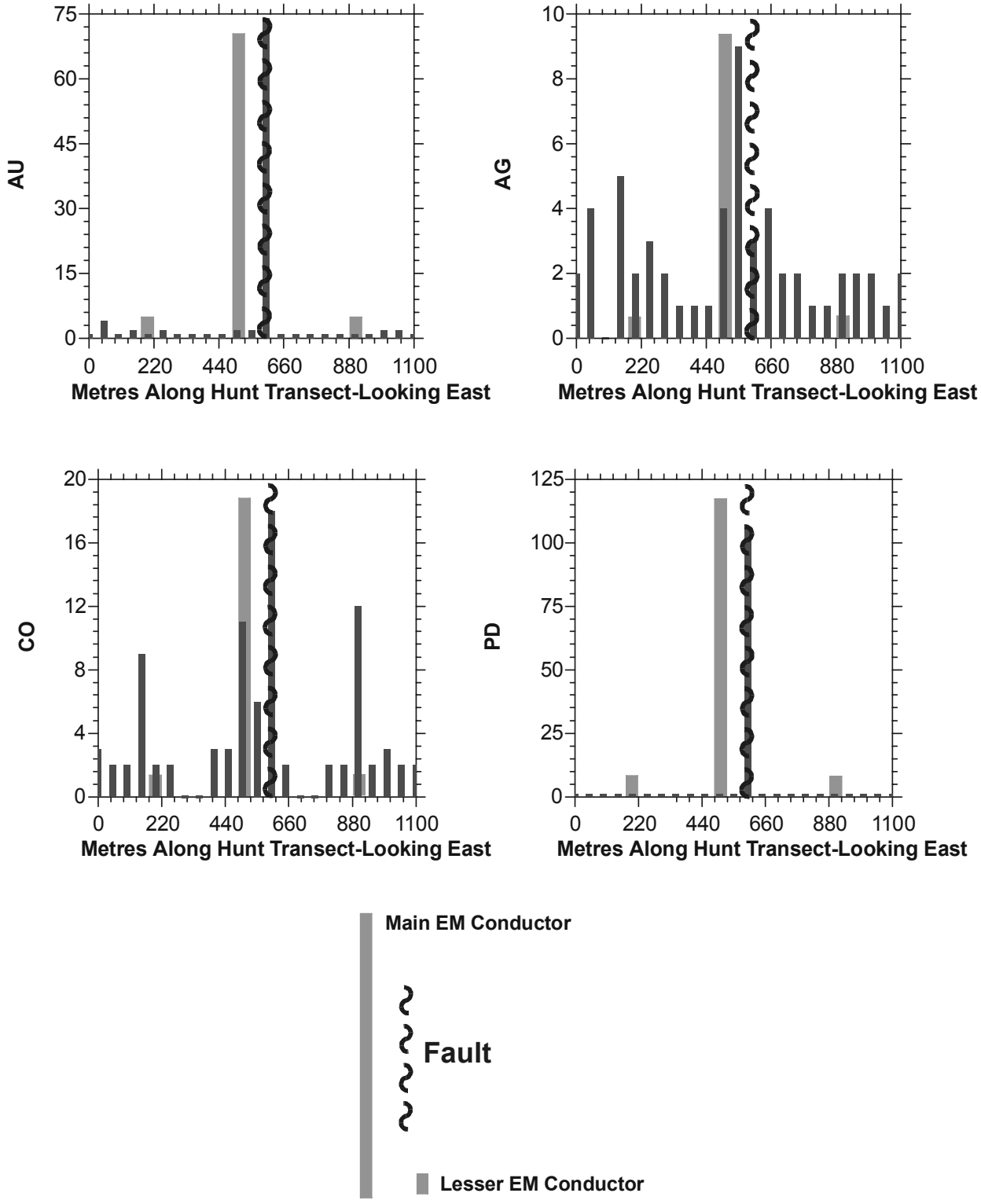

Appendix 7 Continued
Hunt L14E-MMI Response Ratios

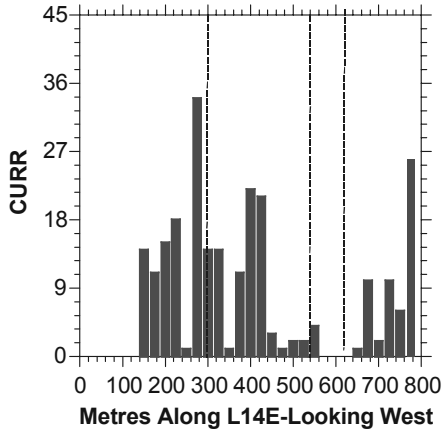

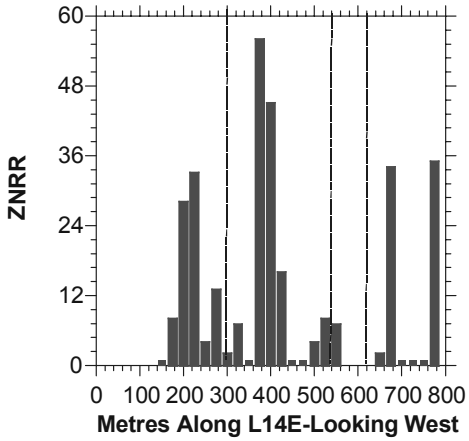

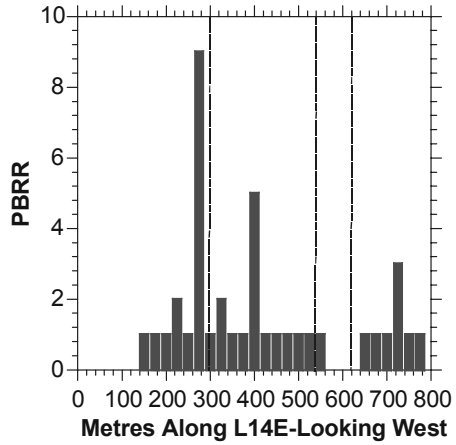

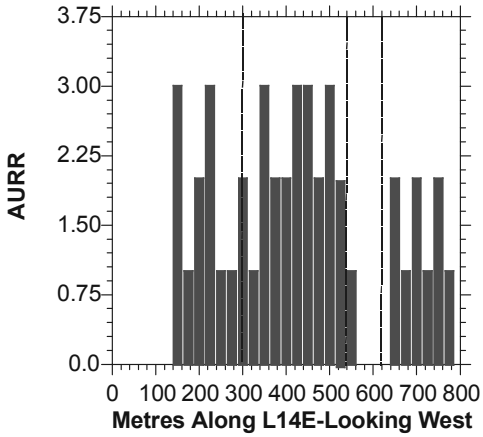

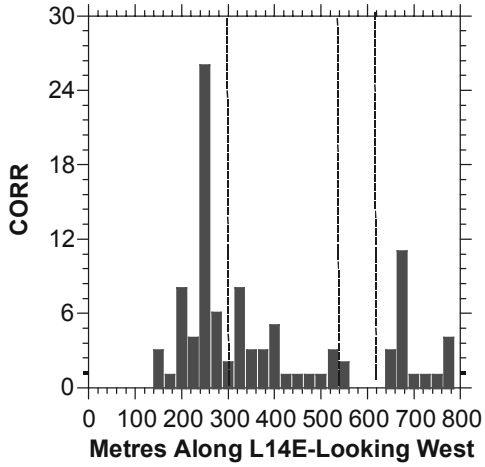

Ground EM Conductor

Appendix 7 Continued
Hunt L14E-MMI Response Ratios

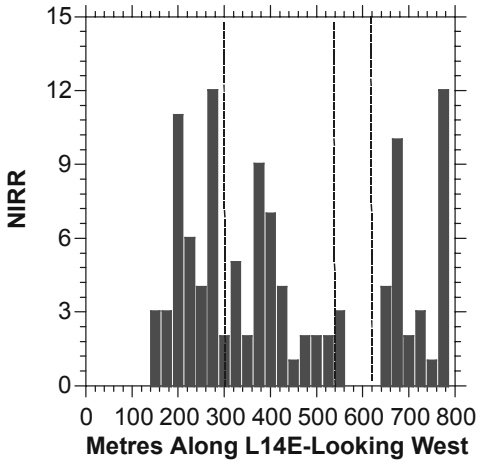

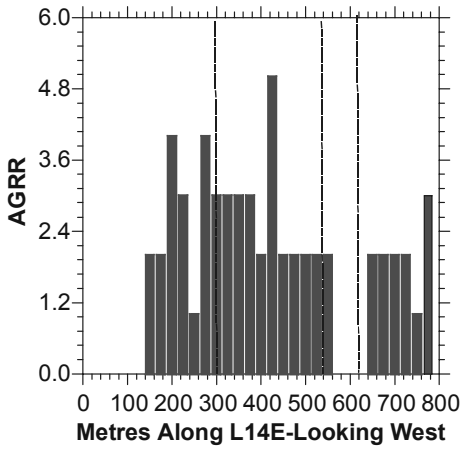

Appendix 7 Continued
Hunt L19E-MMI Response Ratios

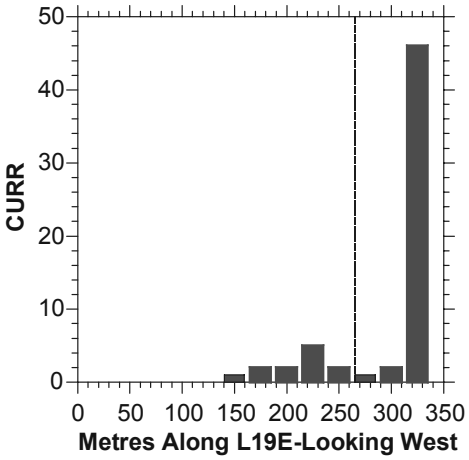

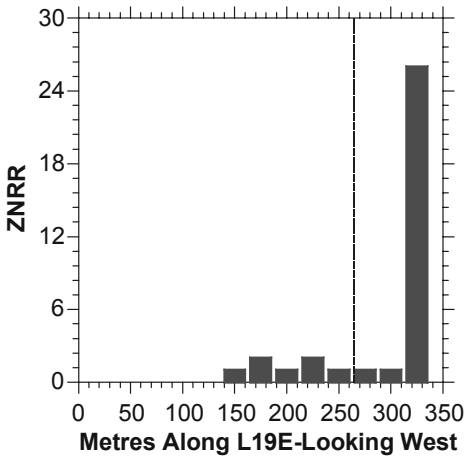

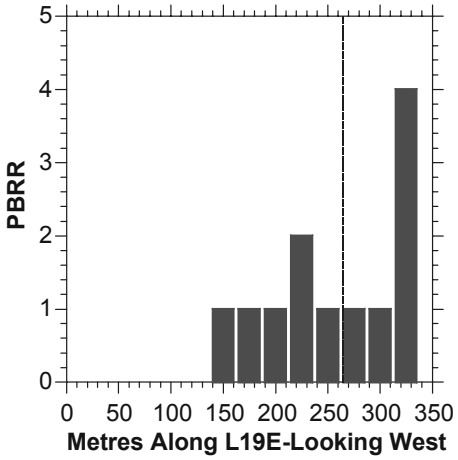

Ground EM Conductor

Appendix 7 Continued
Hunt L19E-MMI Response Ratios

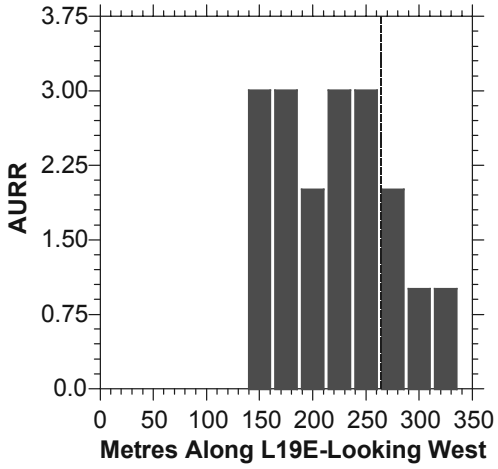

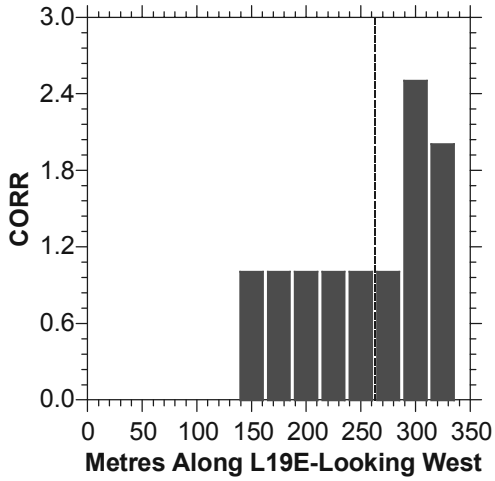

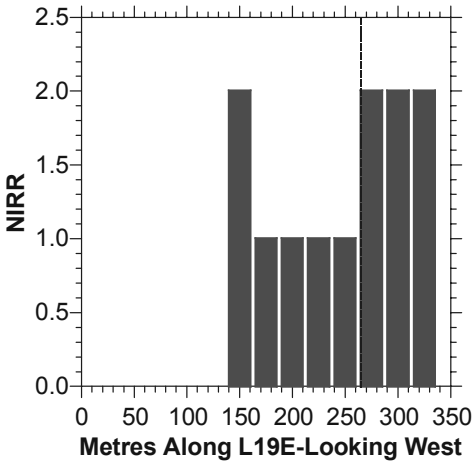

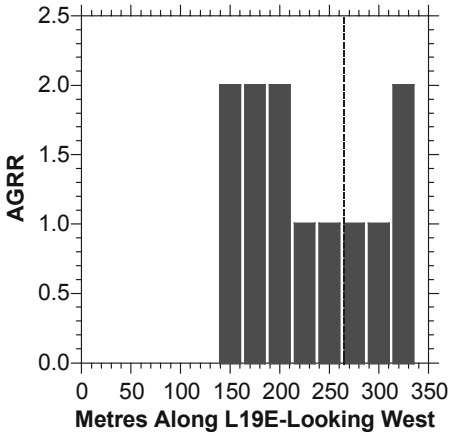

Ground EM Conductor

Appendix 7 Continued
Hunt L23E-MMI Response Ratios

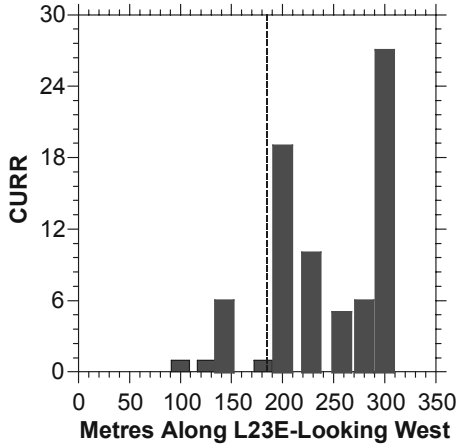

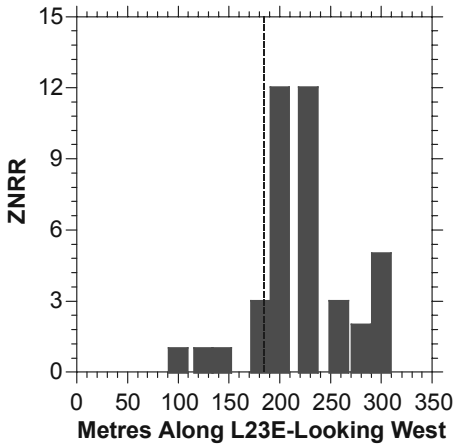

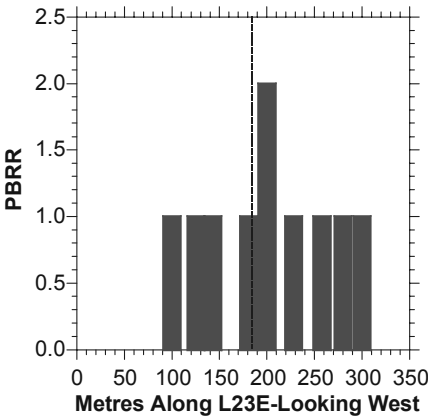

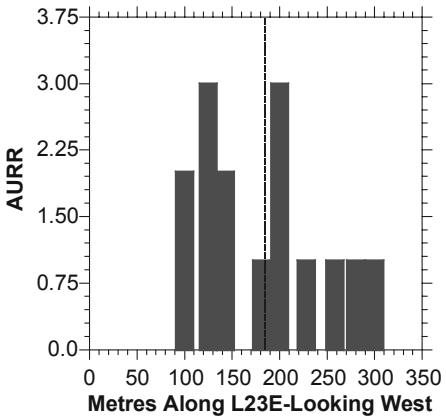

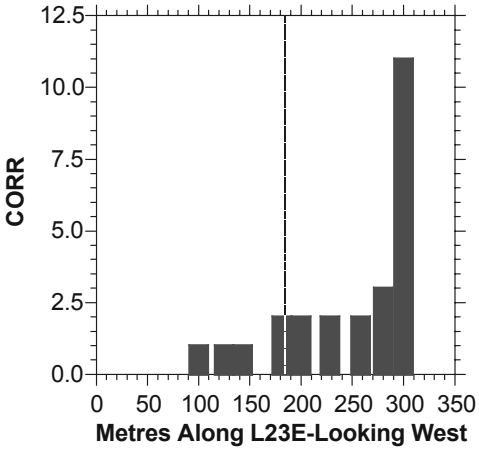

Ground EM Conductor

Appendix 7 Continued
Hunt L23E-MMI Response Ratios

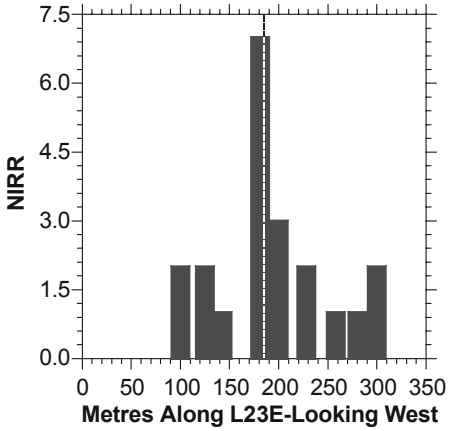

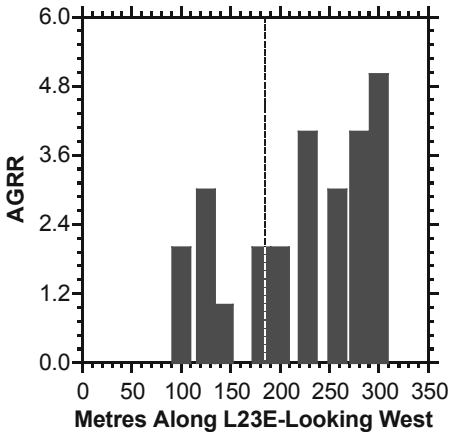

Ground EM Conductor

Appendix 7 Continued
Hunt L29E-MMI Response Ratios

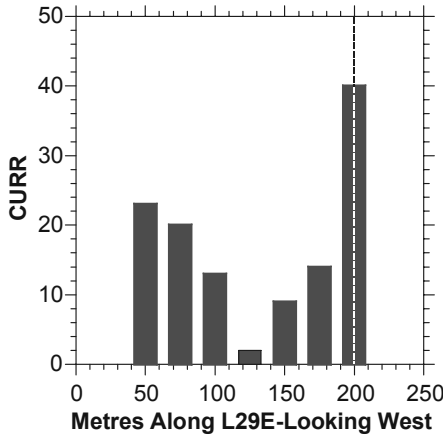

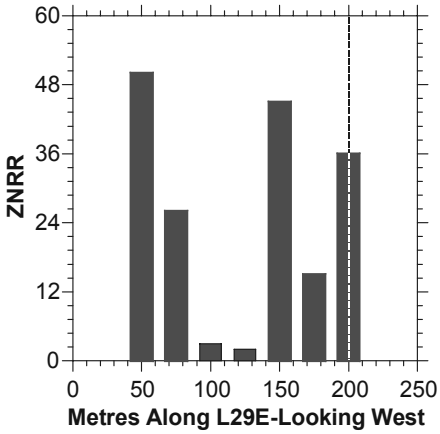

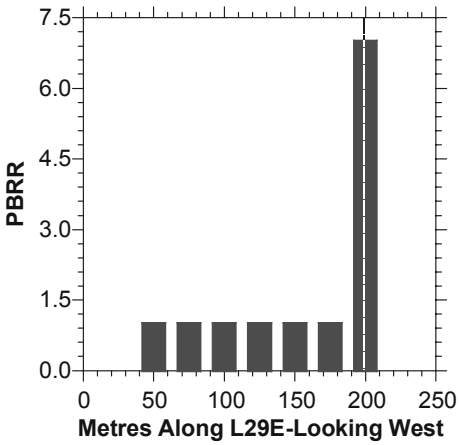

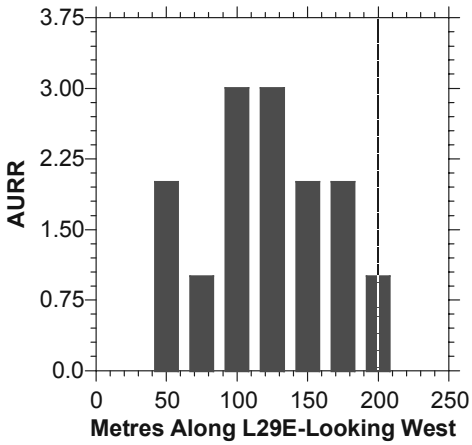

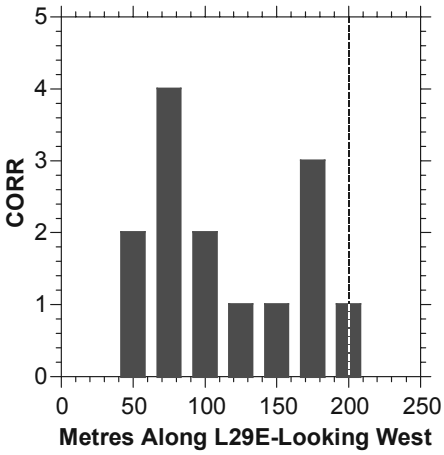

Ground EM Conductor

Appendix 7 Continued
Hunt L29E-MMI Response Ratios

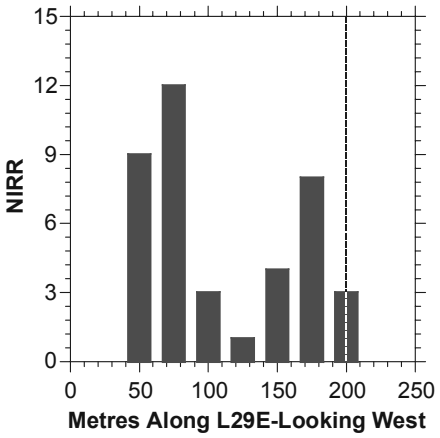

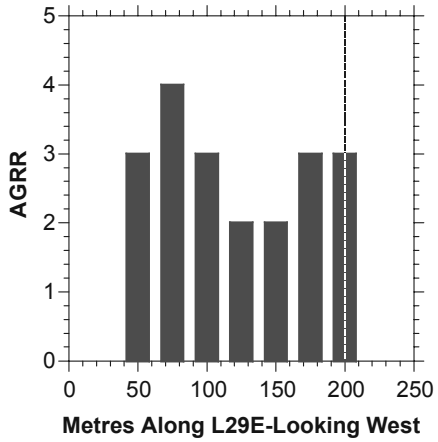

Ground EM Conductor